A Supplementary File for "An Analysis of Quality Indicators Using Approximated Optimal Distributions in a Three-dimensional Objective Space"

Ryoji Tanabe, *Member, IEEE,* and Hisao Ishibuchi, *Fellow, IEEE*

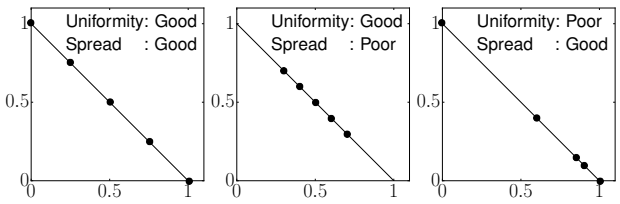

(a) $\boldsymbol{A}_1$ (b) $\boldsymbol{A}_2$ (c) $\boldsymbol{A}_3$

Fig. S.1: Distributions of objective vectors in the three cases for a bi-objective problem. The x and y axes represent f_1 and f_2, respectively. Fig. S.1 was depicted using [S.1] as reference. Since all elements in $\boldsymbol{A}_1$, $\boldsymbol{A}_2$, and $\boldsymbol{A}_3$ are on the Pareto front, they have a good convergence. $\boldsymbol{A}_1$ has good uniformity and spread. While $\boldsymbol{A}_2$ has a good uniformity and a poor spread, $\boldsymbol{A}_3$ has a poor uniformity and a good spread.

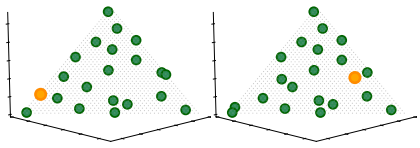

(a) $\boldsymbol{A}_{\mathrm{PD}}^{\mathrm{mod1}}$ (b) $\boldsymbol{A}_{\mathrm{PD}}^{\mathrm{mod2}}$

Fig. S.2: Two modified versions of $\boldsymbol{A}_{\mathrm{PD}}$ for F_{linear}.

S.1. Seven Front Shape Functions

Here, we explain the following seven front shape functions: F_{linear}, F_{convex}, $F_{\mathrm{i\text{-}linear}}$, $F_{\mathrm{i\text{-}concave}}$, $F_{\mathrm{i\text{-}convex}}$, $F_{\mathrm{disconnected}}$, and $F_{\mathrm{c\text{-}concave}}$. For F_{concave}, see Subsection IV-C in the main paper. All front shape functions are based on the method of generating reference vectors presented by Tian et al. [S.2].

A. Linear front shape function F_{linear}

In F_{linear}, the i-th element b_i of $\boldsymbol{b}$ in $\boldsymbol{B}$ is translated into the i-th element a_i of $\boldsymbol{a}$ in $\boldsymbol{A}$ on the linear Pareto front as follows:

$$a_i = b_i, \tag{S.1}$$

R. Tanabe and H. Ishibuchi are with Shenzhen Key Laboratory of Computational Intelligence, University Key Laboratory of Evolving Intelligent Systems of Guangdong Province, Department of Computer Science and Engineering, Southern University of Science and Technology, Shenzhen 518055, China. e-mail: (rt.ryoji.tanabe@gmail.com, hisao@sustech.edu.cn). (Corresponding author: Hisao Ishibuchi)

where b_i is assigned to a_i with no change. Note that the original range of objective values in the Pareto front of DTLZ1 is $[0, 0.5]$. In (S.1), all objective values are in the normalized range $[0, 1]$.

B. Convex front shape function F_{convex}

In F_{convex}, the i-th element b_i of $\boldsymbol{b}$ in $\boldsymbol{B}$ is translated into the i-th element a_i of $\boldsymbol{a}$ in $\boldsymbol{A}$ on the convex Pareto front as follows:

$$\begin{aligned} a_i &= \frac{b_i}{t}, \\ t &= \frac{1}{2}\Big(\delta + 2\,b_m + \sqrt{\delta^2 + 4\delta\,b_m}\Big), \\ \delta &= \left(\sum_{j=1}^{m-1}\sqrt{b_j}\right)^2. \end{aligned} \tag{S.2}$$

C. Three inverted front shape functions $F_{\mathrm{i\text{-}linear}}$, $F_{\mathrm{i\text{-}concave}}$, and $F_{\mathrm{i\text{-}convex}}$

For $F_{\mathrm{i\text{-}linear}}$, $F_{\mathrm{i\text{-}concave}}$, and $F_{\mathrm{i\text{-}convex}}$, first, $\boldsymbol{B}$ is translated into $\boldsymbol{A}$ by F_{linear}, F_{convex}, and F_{concave}, respectively. Then, the i-th element a_i of $\boldsymbol{a}$ in $\boldsymbol{A}$ is further translated as follows:

$$a_i = 1 - a_i. \tag{S.3}$$

D. Disconnected front shape function $F_{\mathrm{disconnected}}$

As mentioned in Subsection IV-A, the disconnected front shape function $F_{\mathrm{disconnected}}$ requires an alternative formulation. The translation operation in (22) is not used when $F_{\mathrm{disconnected}}$ is selected. Thus, the d-dimensional solution $\boldsymbol{\theta}$ is directly translated into the objective vector set $\boldsymbol{A}$.

Similar to other front shape functions, all d elements in $\boldsymbol{\theta}$ are divided into μ vector groups as $(\theta_1, ..., \theta_{1+m-2})^{\mathrm{T}}$, ..., $(\theta_{d-m+2}, ..., \theta_d)^{\mathrm{T}}$. Let $(\theta_i, ..., \theta_{i+m-2})^{\mathrm{T}}$ be $\boldsymbol{y} = (y_1, ..., y_{m-1})^{\mathrm{T}}$ for each $i \in \{1, 1(m-1), 2(m-1), ..., (d-m+2)\}$. In $F_{\mathrm{disconnected}}$, the $(m-1)$-dimensional vector $\boldsymbol{y}$ is directly translated into an m-dimensional objective vector $\boldsymbol{a}$ in $\boldsymbol{A}$ as follows:

$$a_i = \begin{cases} y_i & i < m \\ 2m - \sum_{j=1}^{m-1} y_j\big(1 + \sin(3\pi y_j)\big) & i = m \end{cases}. \tag{S.4}$$

After $\boldsymbol{a}$ has been generated, all elements in $\boldsymbol{a}$ are normalized in $[0, 1]$. To obtain all μ objective vectors in $\boldsymbol{A}$, the same operation is repeatedly applied to $\boldsymbol{y}$ for each $i \in \{1, 1(m-1), 2(m-1), ..., (d-m+2)\}$.

E. Constrained concave front shape function $F_{\text{c-concave}}$

First, $\boldsymbol{B}$ is translated into $\boldsymbol{A}$ by F_{concave}. Then, the constraint violation value $G(\boldsymbol{A})$ is calculated. For each $\boldsymbol{a}$ in $\boldsymbol{A}$, the constraint violation value $g(\boldsymbol{a})$ is calculated as follows:

$$\begin{aligned} g(\boldsymbol{a}) &= \min\big\{g_1(\boldsymbol{a}), g_2(\boldsymbol{a})\big\}, \qquad \text{(S.5)}\\ g_1(\boldsymbol{a}) &= \min_{i\in\{1,\ldots,m\}}\Bigg\{(a_i-1)^2 \\ &\qquad + \sum_{j\in\{1,\ldots,m\}\setminus\{i\}}(a_j^2-\alpha^2)\Bigg\},\\ g_2(\boldsymbol{a}) &= \sum_{i\in\{1,\ldots,m\}}\left(a_i-\frac{1}{\sqrt{m}}\right)^2-\alpha^2, \end{aligned}$$

where $\boldsymbol{a}$ is infeasible if $g(\boldsymbol{a})>0$ in (S.5).

In our study, the constraint violation value $G(\boldsymbol{A})$ is determined based on the number of infeasible objective vectors in $\boldsymbol{A}$. $\boldsymbol{A}$ is said to a feasible objective vector set iff all objective vectors in $\boldsymbol{A}$ are feasible. Otherwise, $\boldsymbol{A}$ is said to an infeasible objective vector set (i.e., at least one objective vector in $\boldsymbol{A}$ is infeasible). We set $G(\boldsymbol{A})$ to 0 for all feasible objective vector sets and an infinitely large value for all infeasible objective vector sets.

S.2. Method of generating the reference vector set

Here, we explain how we generated the reference vector set $\boldsymbol{R}$. Simply, we generated $\boldsymbol{R}$ by applying each front shape function F to the weight vector set $\boldsymbol{W}$ as follows:

$$\boldsymbol{R} = F(\boldsymbol{W}),$$

where we generated $\boldsymbol{W}$ using simplex-lattice design [S.3].

For example, in F_{concave}, the i-th element w_i of $\boldsymbol{w}$ in $\boldsymbol{W}$ is translated into the i-th element r_i of $\boldsymbol{r}$ in $\boldsymbol{R}$ on the concave Pareto front as follows:

$$r_i = \frac{w_i}{t},$$

where $t = \sqrt{\sum_{j=1}^{m} w_j^2}$. This translation is the same as F_{concave} in (24) described in Subsection IV-C. We generated $\boldsymbol{R}$ for other front shape functions (F_{linear}, ..., $F_{\text{c-concave}}$) in a same manner. It should be noted that all reference vectors in $\boldsymbol{R}$ are shown in Figs. 2–9.

S.3. Comparison of L-SHADE and the analytical approach for $m = 2$

Here, we examine how well L-SHADE approximates the optimal μ-distributions for $m = 2$. We compare L-SHADE to the analytical approach that approximates the optimal μ-distributions for HV for $m = 2$ [S.4] (see Subsection III-B). As mentioned in Section IV, our formulation for $m = 2$ is almost the same as the formulation in (19). In addition, front shape functions used in [S.4] are only for $m = 2$. For these reasons, we used the formulation in (19) in this comparison.

Table S.1 shows error values between $\text{HV}(\boldsymbol{A}^{\text{best}})$ and $\text{HV}(\boldsymbol{A}^{\text{analytical}})$ on the front shape functions of ZDT1, ZDT2, ZDT3, DTLZ1, DTLZ2, and DTLZ7 with $m = 2$ (F_{ZDT1}, F_{ZDT2}, F_{ZDT3}, F_{DTLZ1}, F_{DTLZ2}, and F_{DTLZ7}). The front shape functions of ZDT1 and ZDT4 are the same. The front shape function of ZDT6 is the shifted version of the front shape function of ZDT2. The front shape functions of DTLZ3 and DTLZ4 are the same as the front shape function of DTLZ2. For these reasons, we removed the results of ZDT4, ZDT6, DTLZ3, and DTLZ4. For each front shape function, we compare the best objective vector set found by L-SHADE among 31 runs $\boldsymbol{A}^{\text{best}}$ to the objective vector set $\boldsymbol{A}^{\text{analytical}}$ obtained by the analytical approach in [S.4]. We downloaded data of $\boldsymbol{A}^{\text{analytical}}$ from the supplementary website of [S.4] (see Subsection III-B). In this experiment, μ was set to 2, 3, 4, 5, 10, 20, 50, and 100. We calculated the error value of $\boldsymbol{A}^{\text{best}}$ as follows: $\text{error}(\boldsymbol{A}^{\text{best}}) = \text{HV}(\boldsymbol{A}^{\text{analytical}}) - \text{HV}(\boldsymbol{A}^{\text{best}})$. A positive $\text{error}(\boldsymbol{A}^{\text{best}})$ value means that the quality of $\boldsymbol{A}^{\text{best}}$ is worse than that of $\boldsymbol{A}^{\text{analytical}}$, and vice versa. Data of $\boldsymbol{A}^{\text{best}}$ obtained in our experiments can be downloaded from the supplementary website (https://sites.google.com/view/optmudist).

TABLE S.1: Error values between $\text{HV}(\boldsymbol{A}^{\text{analytical}})$ and $\text{HV}(\boldsymbol{A}^{\text{best}})$ on F_{ZDT1}, F_{ZDT2}, F_{ZDT3}, F_{DTLZ1}, F_{DTLZ2}, and F_{DTLZ7} with $m = 2$.

μ	F_{ZDT1}	F_{ZDT2}	F_{ZDT3}	F_{DTLZ1}	F_{DTLZ2}	F_{DTLZ7}
2	0.0e+00	0.0e+00	-1.8e-02	0.0e+00	0.0e+00	0.0e+00
3	0.0e+00	0.0e+00	-3.9e-03	0.0e+00	0.0e+00	0.0e+00
4	0.0e+00	0.0e+00	-1.5e-03	0.0e+00	0.0e+00	0.0e+00
5	0.0e+00	0.0e+00	-1.5e-03	0.0e+00	0.0e+00	0.0e+00
10	1.0e-06	0.0e+00	-2.7e-05	0.0e+00	1.0e-06	-2.2e-03
20	6.0e-06	1.0e-05	-5.0e-06	3.0e-06	1.9e-05	-2.9e-03
50	7.4e-05	5.7e-05	5.1e-05	1.5e-05	6.7e-05	2.8e-04
100	1.1e-04	1.2e-04	6.8e-05	2.8e-05	-2.7e-04	4.0e-06

As seen from Table S.1, $\boldsymbol{A}^{\text{best}}$ and $\boldsymbol{A}^{\text{analytical}}$ have exactly the same quality for $\mu \leq 5$ on all front shape functions. The error values increase with the μ on F_{ZDT1}, F_{ZDT2}, and F_{DTLZ1}. This is simply because the dimensionality d of the search space of L-SHADE increases exponentially with μ. However, we are interested in the approximated optimal μ-distribution with small μ values so that we visually examine the distributions of objective vectors. When the size of the approximated optimal μ-distribution is large, its distribution is unclear. In addition, L-SHADE finds better approximations of the optimal μ-distributions for HV on ZDT3 with $\mu \in \{2, 3, 4, 5, 10, 20\}$, DTLZ2 with $\mu = 100$, and DTLZ7 with $\mu \in \{10, 20\}$. Based on the above-mentioned results, we conclude that L-SHADE can find the approximated optimal μ-distribution for HV with acceptable quality for $m = 2$.

S.4. Diversity comparison indicator (DCI) [S.5]

We explain the diversity comparison indicator (DCI) [S.5]. DCI compares M objective vector sets $\boldsymbol{A}_1$, ..., $\boldsymbol{A}_M$ in a relative manner. DCI divides the objective vector space into div^m grids based on all objective vectors in $\boldsymbol{A}_1$, ..., $\boldsymbol{A}_M$. DCI considers only hyperboxes that contain at least one objective vector in $\boldsymbol{A}_1$, ..., $\boldsymbol{A}_M$. For each $i \in \{1, ..., M\}$, the DCI value of $\boldsymbol{A}_i$ is calculated based on the number of objective vectors in $\boldsymbol{A}_i$ in each hyperbox. The DCI value of $\boldsymbol{A}_i$ is large when objective vectors in $\boldsymbol{A}_i$ cover or are close to all the hyperboxes. The range of the DCI value is $[0, 1]$. A large DCI

value indicates that $\boldsymbol{A}_i$ has a good diversity among $\boldsymbol{A}_1$, ..., $\boldsymbol{A}_M$.

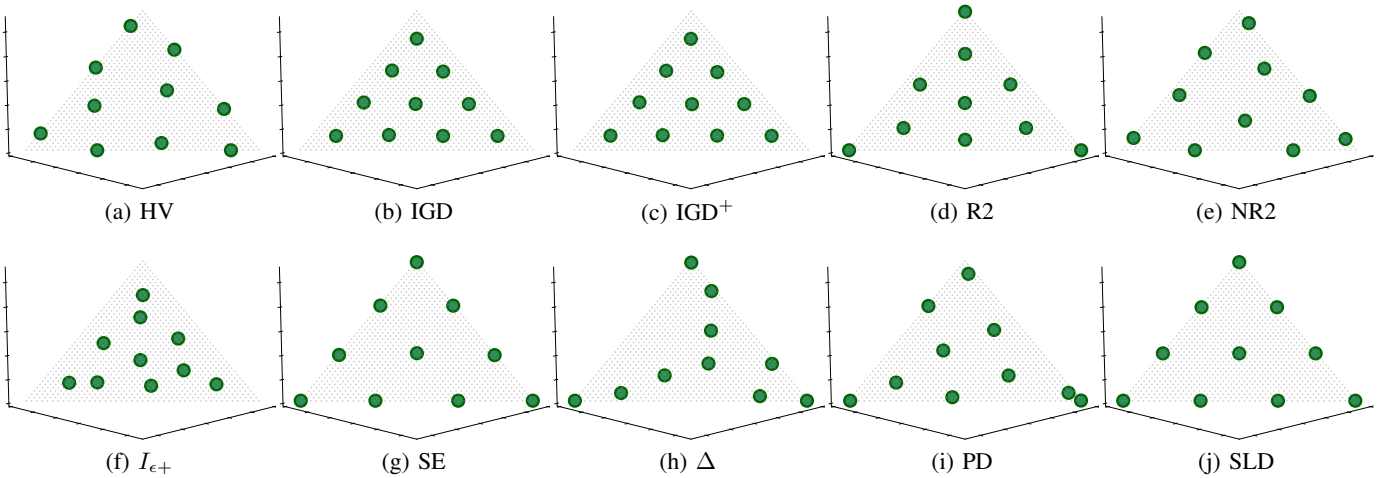

(a) HV (b) IGD (c) IGD$^+$ (d) R2 (e) NR2

(f) $I_{\epsilon+}$ (g) SE (h) Δ (i) PD (j) SLD

Fig. S.3: Approximated optimal μ-distributions with $\mu = 10$ on F_{linear} (the linear Pareto front).

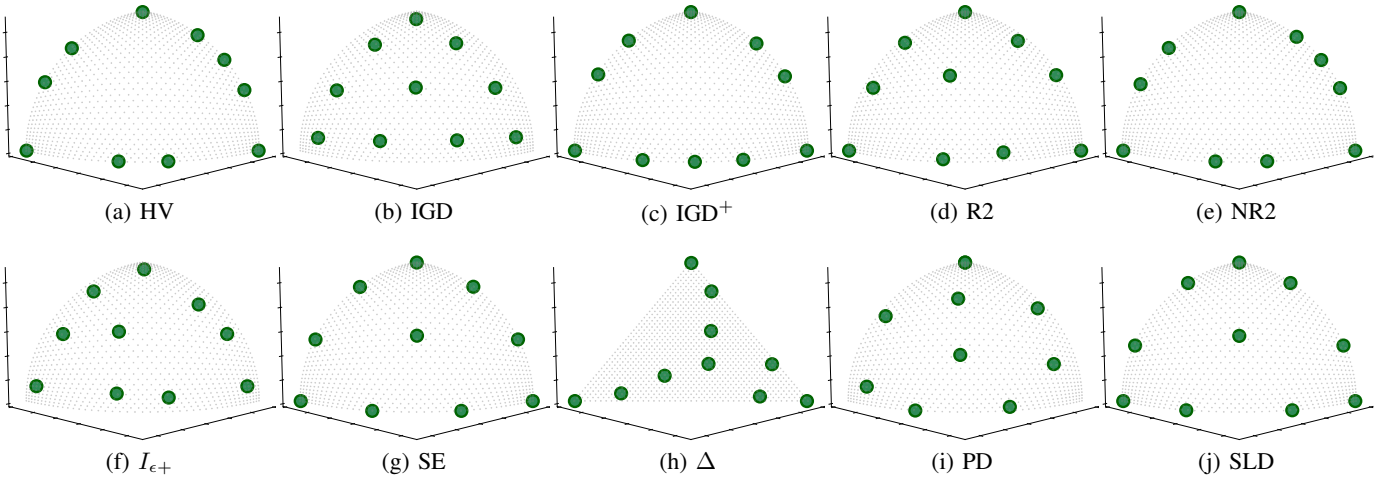

(a) HV (b) IGD (c) IGD$^+$ (d) R2 (e) NR2

(f) $I_{\epsilon+}$ (g) SE (h) Δ (i) PD (j) SLD

Fig. S.4: Approximated optimal μ-distributions with $\mu = 10$ on F_{concave} (the concave Pareto front).

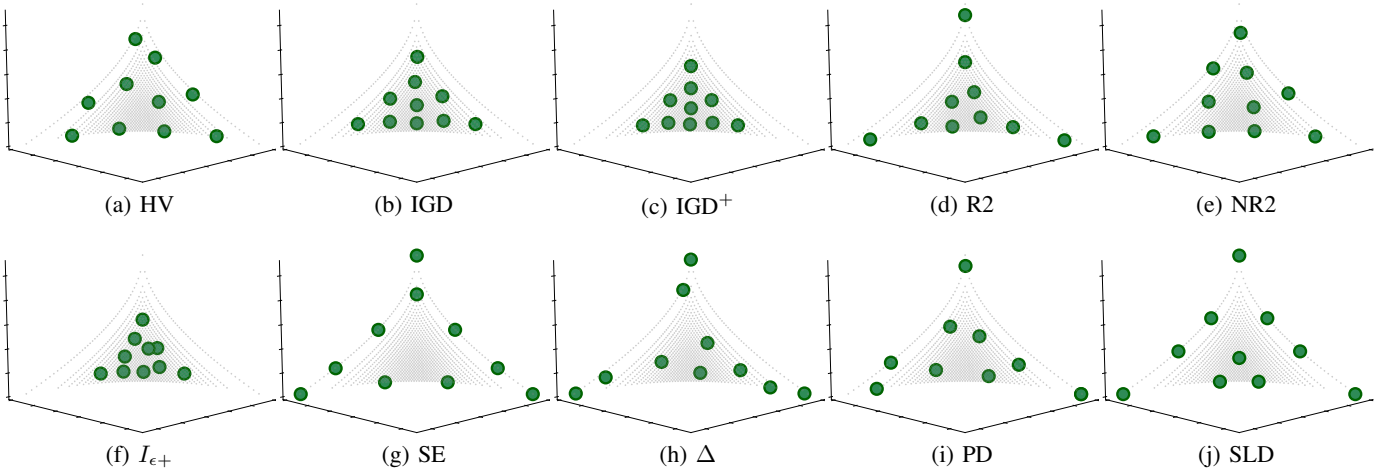

(a) HV (b) IGD (c) IGD$^+$ (d) R2 (e) NR2

(f) $I_{\epsilon+}$ (g) SE (h) Δ (i) PD (j) SLD

Fig. S.5: Approximated optimal μ-distributions with $\mu = 10$ on F_{convex} (the convex Pareto front).

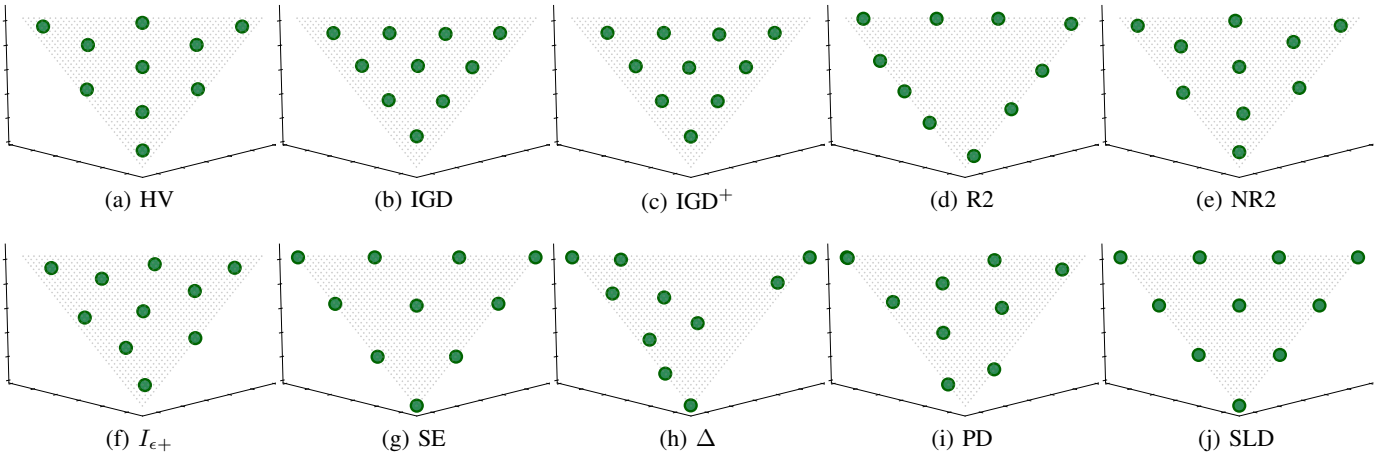

(a) HV (b) IGD (c) IGD$^+$ (d) R2 (e) NR2

(f) $I_{\epsilon+}$ (g) SE (h) Δ (i) PD (j) SLD

Fig. S.6: Approximated optimal μ-distributions with $\mu = 10$ on $F_{\text{i-linear}}$ (the inverted linear Pareto front).

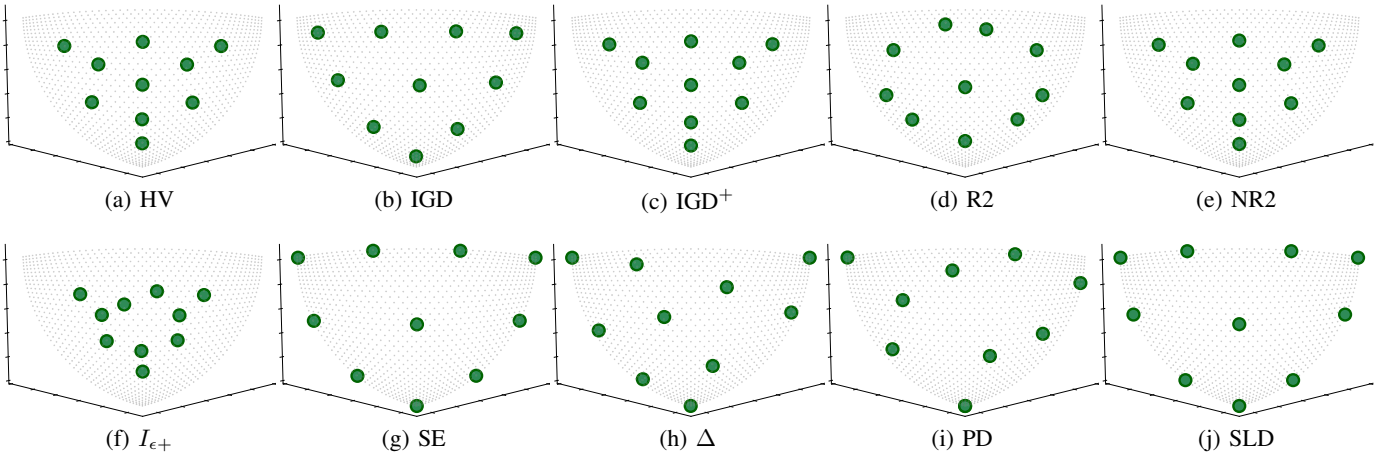

(a) HV (b) IGD (c) IGD$^+$ (d) R2 (e) NR2

(f) $I_{\epsilon+}$ (g) SE (h) Δ (i) PD (j) SLD

Fig. S.7: Approximated optimal μ-distributions with $\mu = 10$ on $F_{\text{i-convex}}$ (the inverted convex Pareto front).

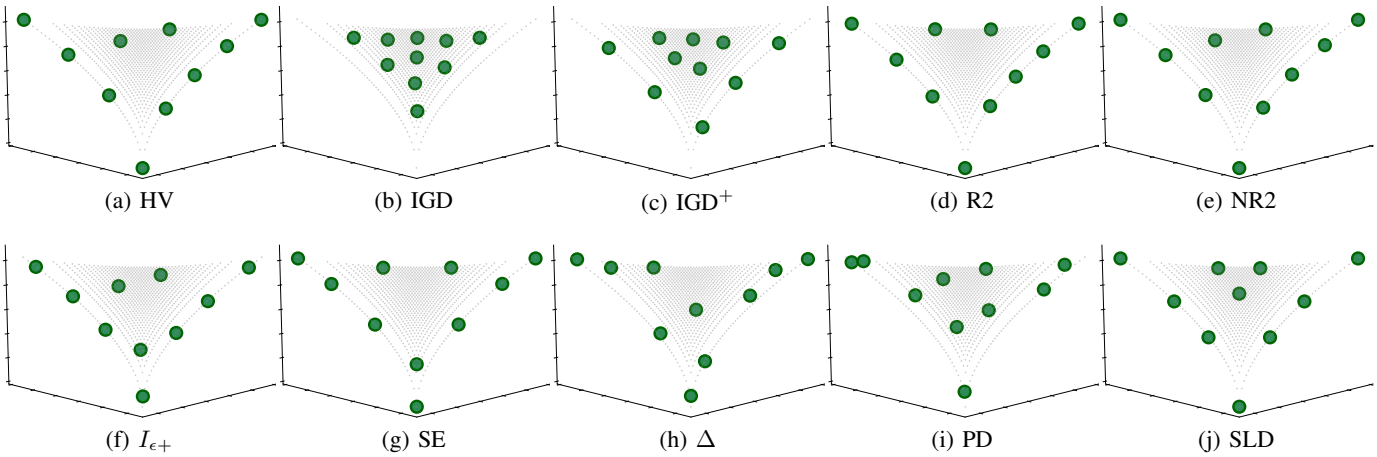

(a) HV (b) IGD (c) IGD$^+$ (d) R2 (e) NR2

(f) $I_{\epsilon+}$ (g) SE (h) Δ (i) PD (j) SLD

Fig. S.8: Approximated optimal μ-distributions with $\mu = 10$ on $F_{\text{i-concave}}$ (the inverted concave Pareto front).

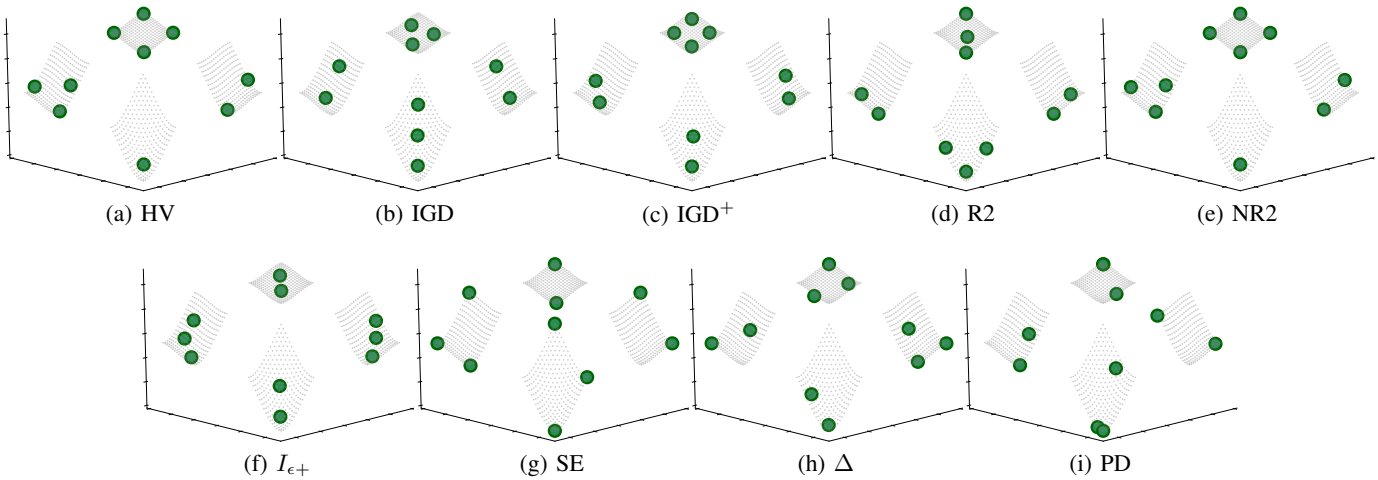

(a) HV (b) IGD (c) IGD$^+$ (d) R2 (e) NR2

(f) $I_{\epsilon+}$ (g) SE (h) Δ (i) PD

Fig. S.9: Approximated optimal μ-distributions with $\mu = 10$ on $F_{\text{disconnected}}$ (the disconnected Pareto front).

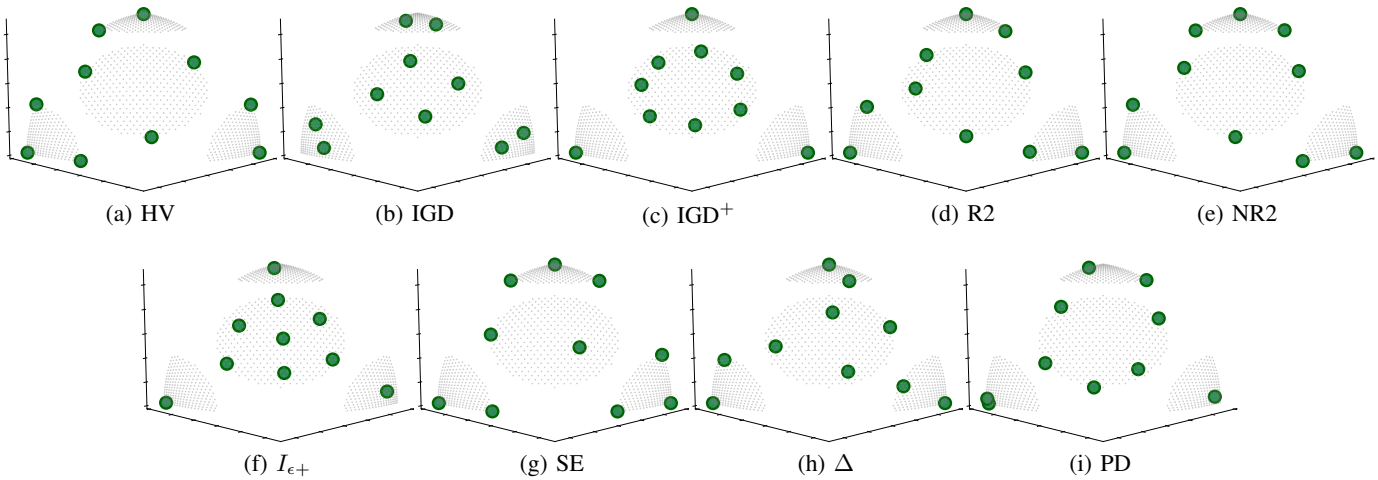

(a) HV (b) IGD (c) IGD$^+$ (d) R2 (e) NR2

(f) $I_{\epsilon+}$ (g) SE (h) Δ (i) PD

Fig. S.10: Approximated optimal μ-distributions with $\mu = 10$ on $F_{\text{c-concave}}$ (the constrained concave Pareto front).

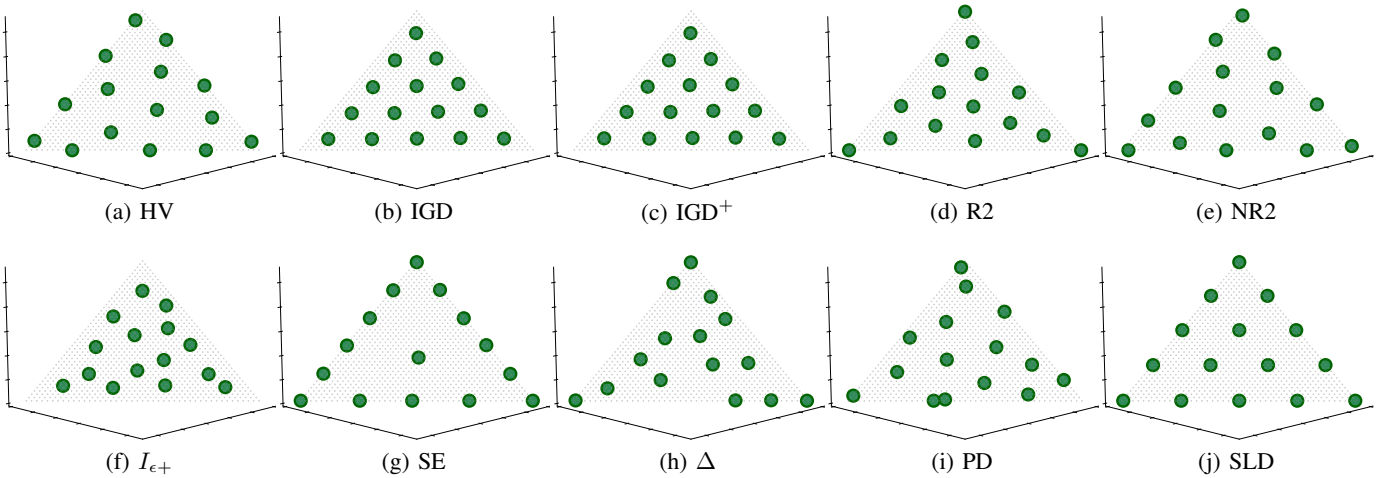

(a) HV (b) IGD (c) IGD$^+$ (d) R2 (e) NR2

(f) $I_{\epsilon+}$ (g) SE (h) Δ (i) PD (j) SLD

Fig. S.11: Approximated optimal μ-distributions with $\mu = 15$ on F_{linear} (the linear Pareto front).

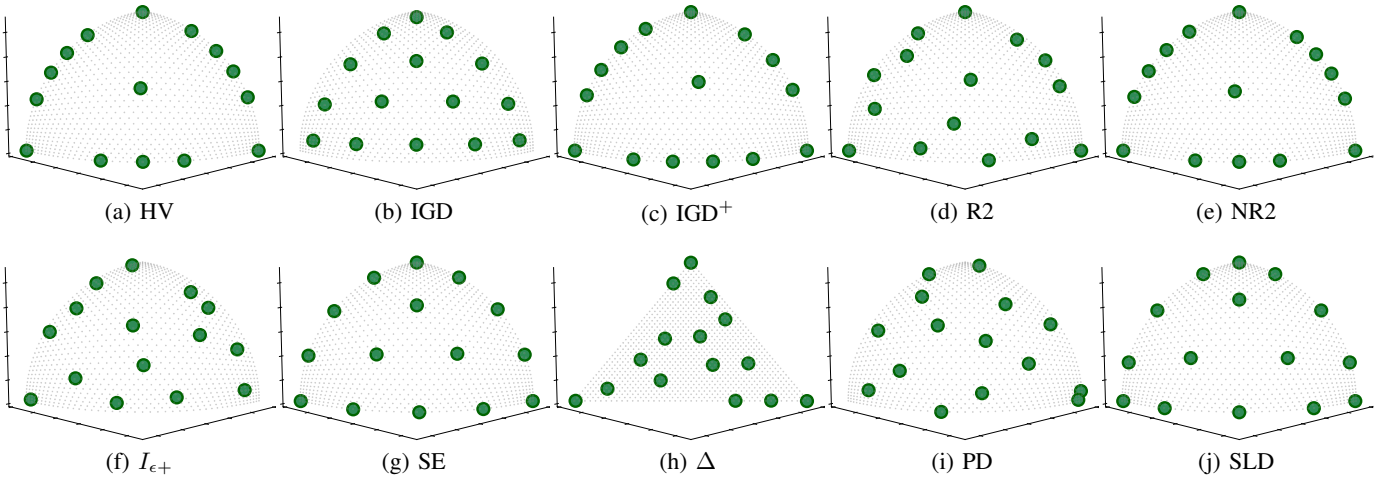

(a) HV (b) IGD (c) IGD$^+$ (d) R2 (e) NR2

(f) $I_{\epsilon+}$ (g) SE (h) Δ (i) PD (j) SLD

Fig. S.12: Approximated optimal μ-distributions with $\mu = 15$ on F_{concave} (the concave Pareto front).

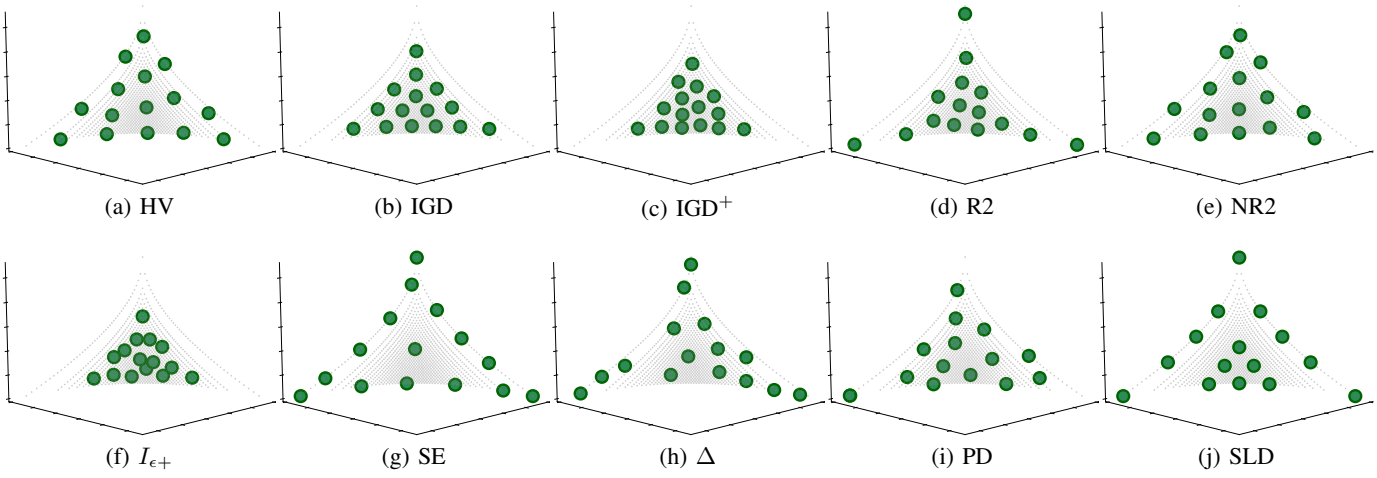

(a) HV (b) IGD (c) IGD$^+$ (d) R2 (e) NR2

(f) $I_{\epsilon+}$ (g) SE (h) Δ (i) PD (j) SLD

Fig. S.13: Approximated optimal μ-distributions with $\mu = 15$ on F_{convex} (the convex Pareto front).

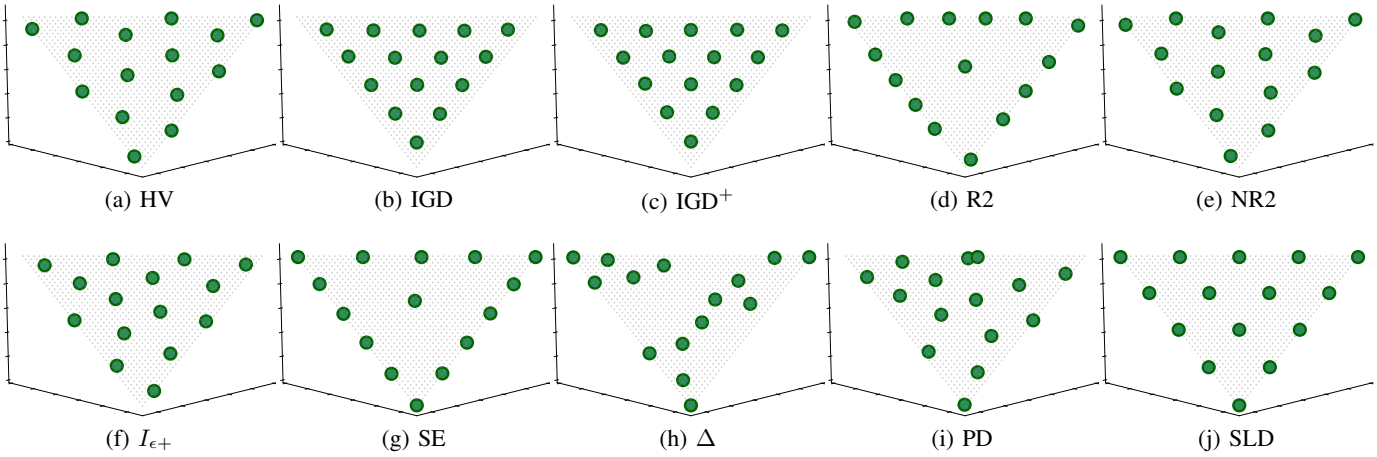

(a) HV (b) IGD (c) IGD$^+$ (d) R2 (e) NR2

(f) $I_{\epsilon+}$ (g) SE (h) Δ (i) PD (j) SLD

Fig. S.14: Approximated optimal μ-distributions with $\mu = 15$ on $F_{\text{i-linear}}$ (the inverted linear Pareto front).

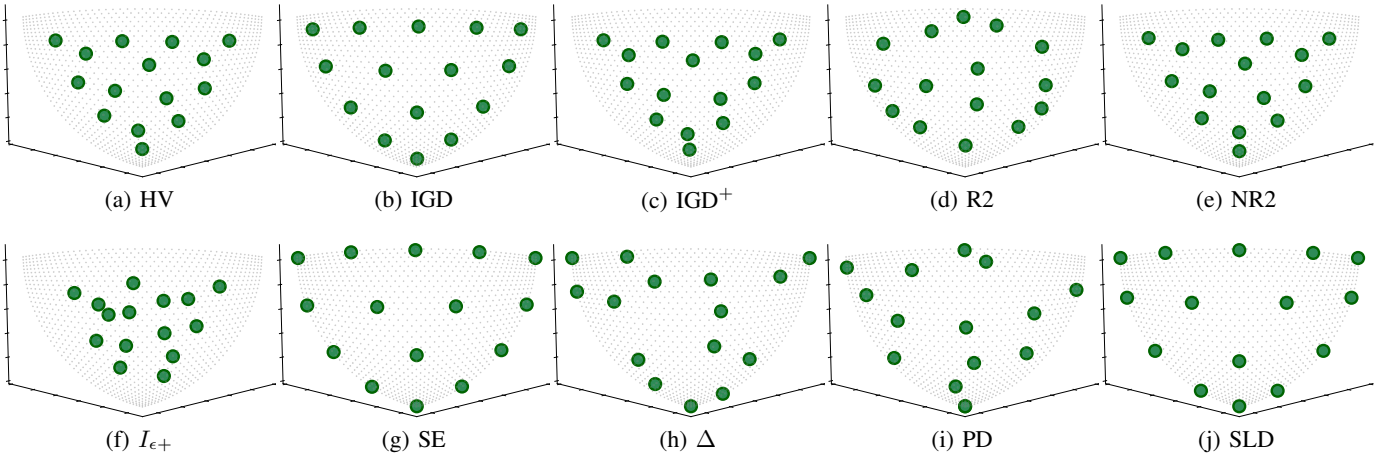

(a) HV (b) IGD (c) IGD$^+$ (d) R2 (e) NR2

(f) $I_{\epsilon+}$ (g) SE (h) Δ (i) PD (j) SLD

Fig. S.15: Approximated optimal μ-distributions with $\mu = 15$ on $F_{\text{i-convex}}$ (the inverted convex Pareto front).

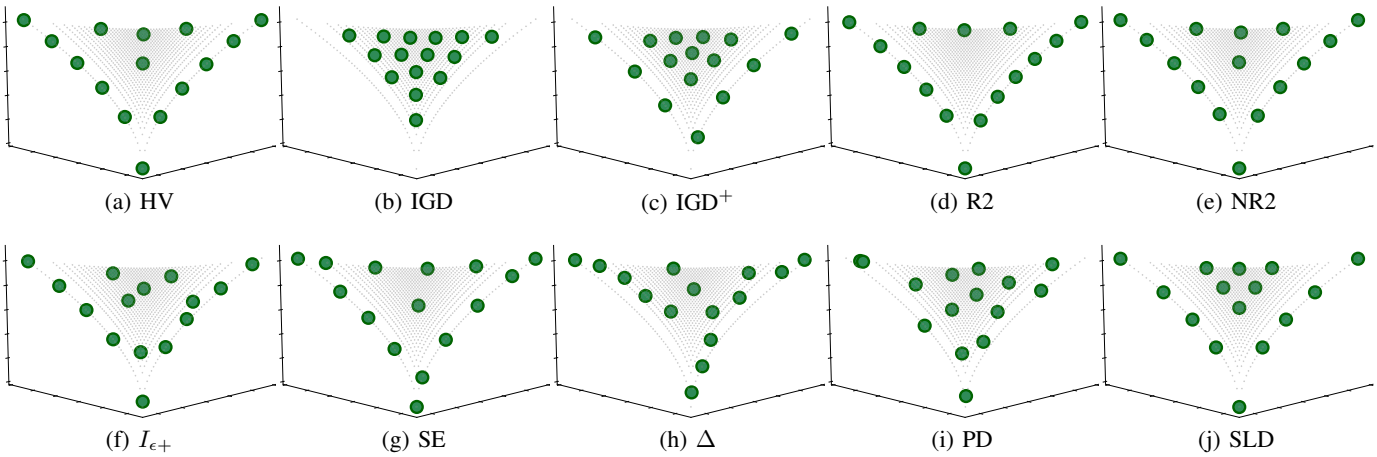

(a) HV (b) IGD (c) IGD$^+$ (d) R2 (e) NR2

(f) $I_{\epsilon+}$ (g) SE (h) Δ (i) PD (j) SLD

Fig. S.16: Approximated optimal μ-distributions with $\mu = 15$ on $F_{\text{i-concave}}$ (the inverted concave Pareto front).

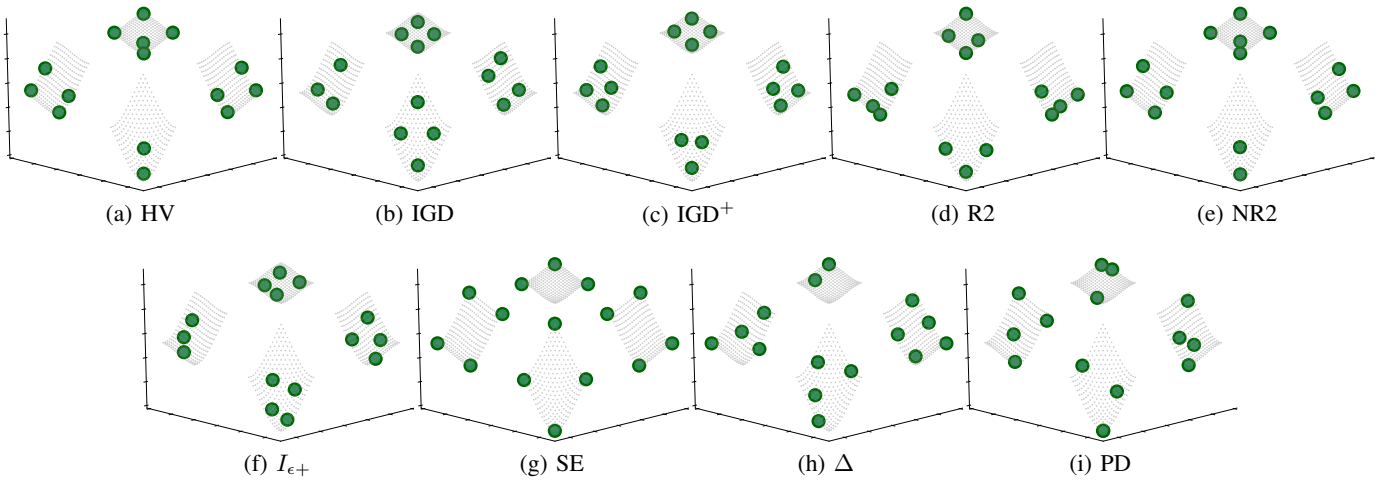

(a) HV (b) IGD (c) IGD$^+$ (d) R2 (e) NR2

(f) $I_{\epsilon+}$ (g) SE (h) Δ (i) PD

Fig. S.17: Approximated optimal μ-distributions with $\mu = 15$ on $F_{\text{disconnected}}$ (the disconnected Pareto front).

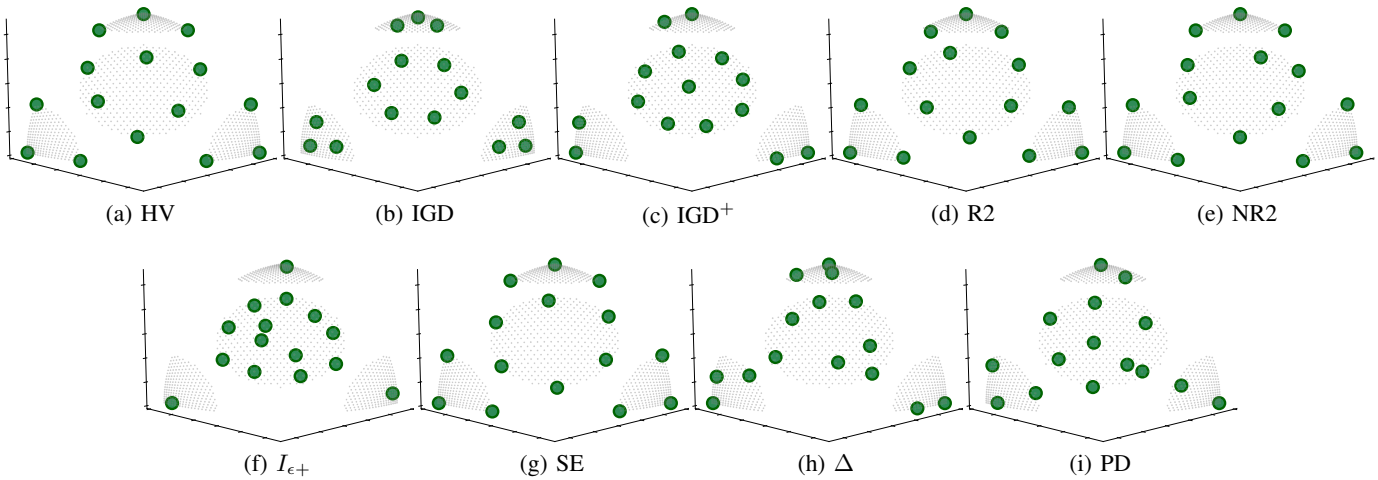

(a) HV (b) IGD (c) IGD$^+$ (d) R2 (e) NR2

(f) $I_{\epsilon+}$ (g) SE (h) Δ (i) PD

Fig. S.18: Approximated optimal μ-distributions with $\mu = 15$ on $F_{\text{c-concave}}$ (the constrained concave Pareto front).

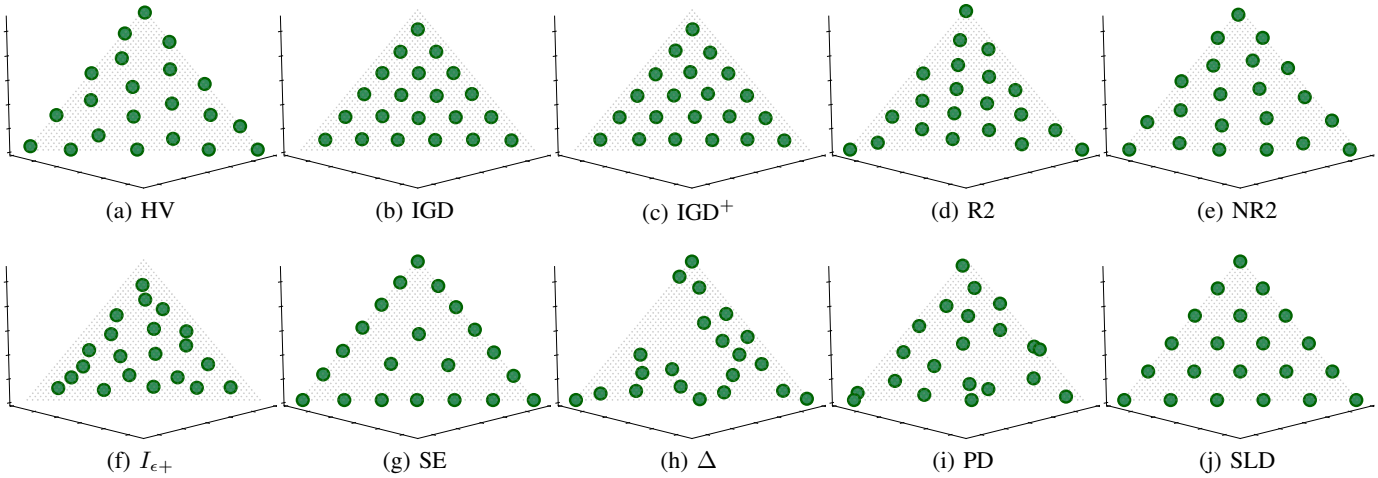

(a) HV (b) IGD (c) IGD$^+$ (d) R2 (e) NR2

(f) $I_{\epsilon+}$ (g) SE (h) Δ (i) PD (j) SLD

Fig. S.19: Approximated optimal μ-distributions with $\mu = 21$ on F_{linear} (the linear Pareto front).

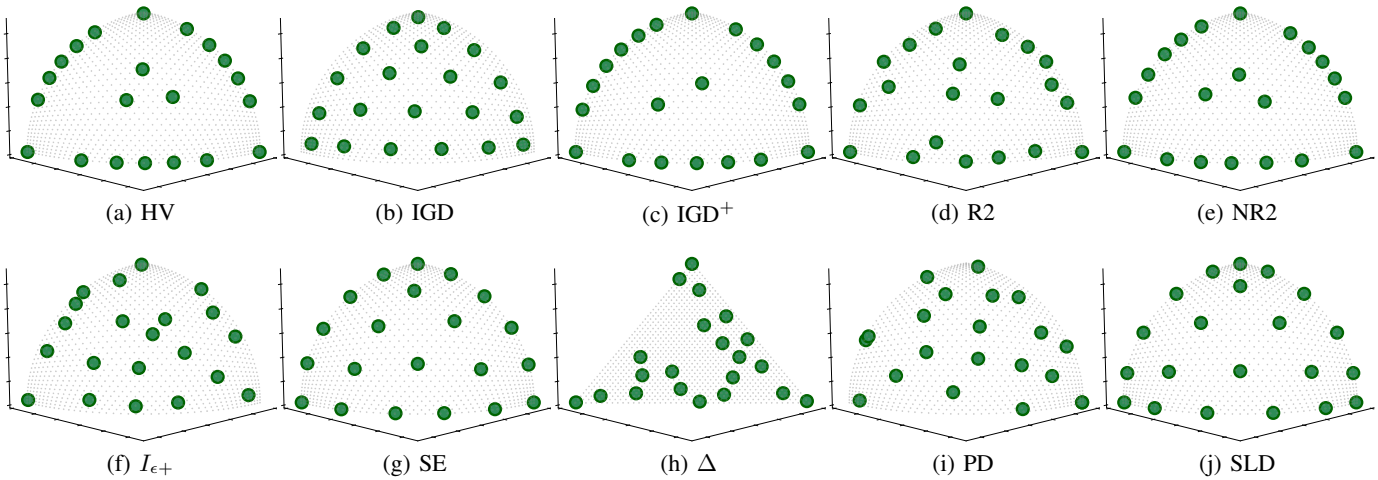

(a) HV (b) IGD (c) IGD$^+$ (d) R2 (e) NR2

(f) $I_{\epsilon+}$ (g) SE (h) Δ (i) PD (j) SLD

Fig. S.20: Approximated optimal μ-distributions with $\mu = 21$ on F_{concave} (the concave Pareto front).

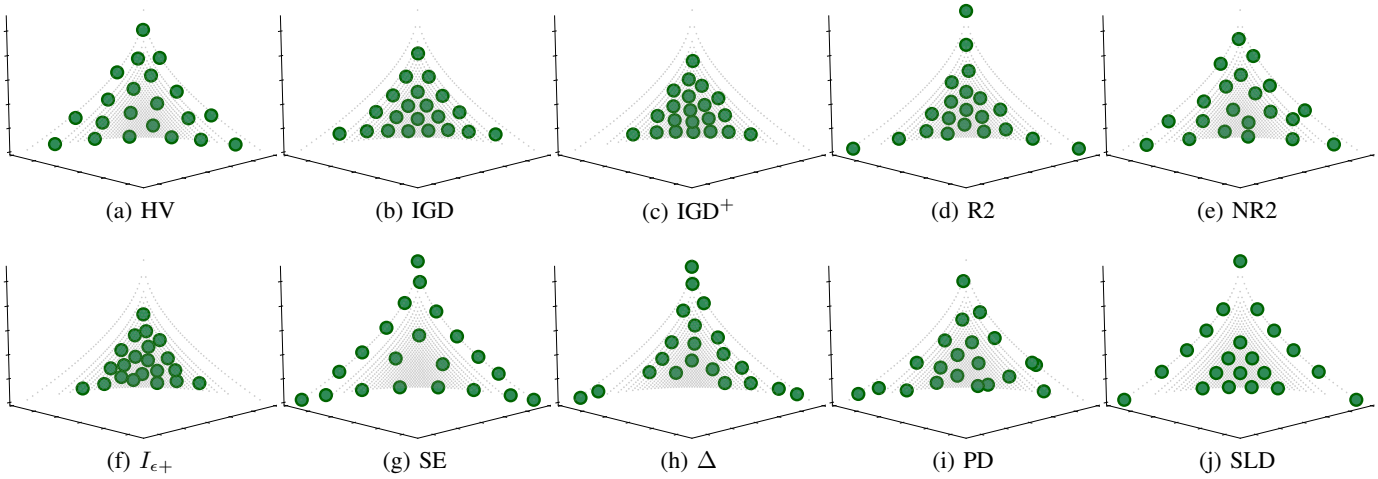

(a) HV (b) IGD (c) IGD$^+$ (d) R2 (e) NR2

(f) $I_{\epsilon+}$ (g) SE (h) Δ (i) PD (j) SLD

Fig. S.21: Approximated optimal μ-distributions with $\mu = 21$ on F_{convex} (the convex Pareto front).

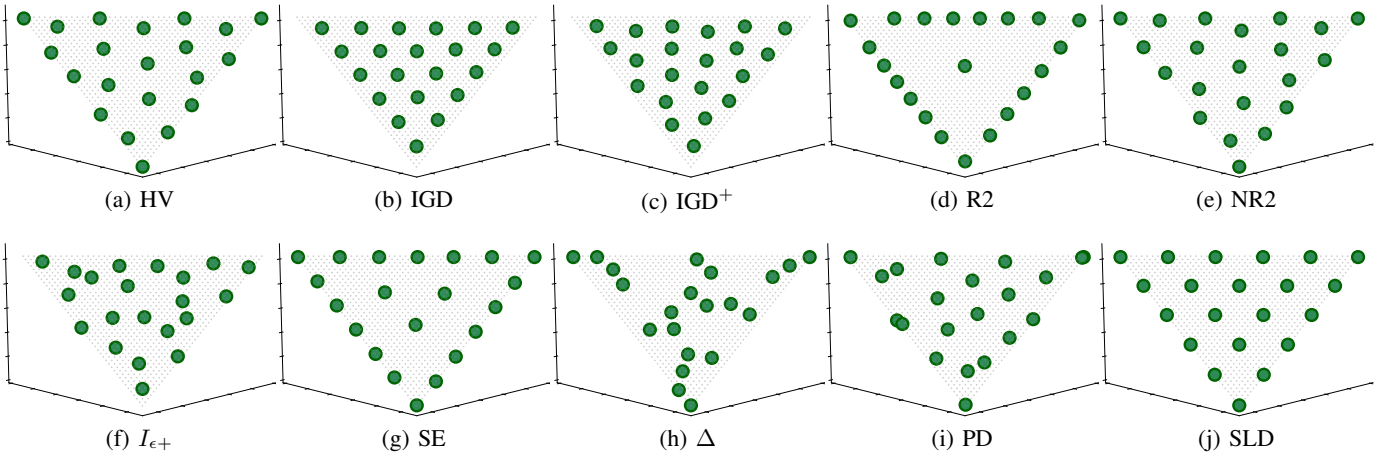

(a) HV (b) IGD (c) IGD$^+$ (d) R2 (e) NR2

(f) $I_{\epsilon+}$ (g) SE (h) Δ (i) PD (j) SLD

Fig. S.22: Approximated optimal μ-distributions with $\mu = 21$ on $F_{\text{i-linear}}$ (the inverted linear Pareto front).

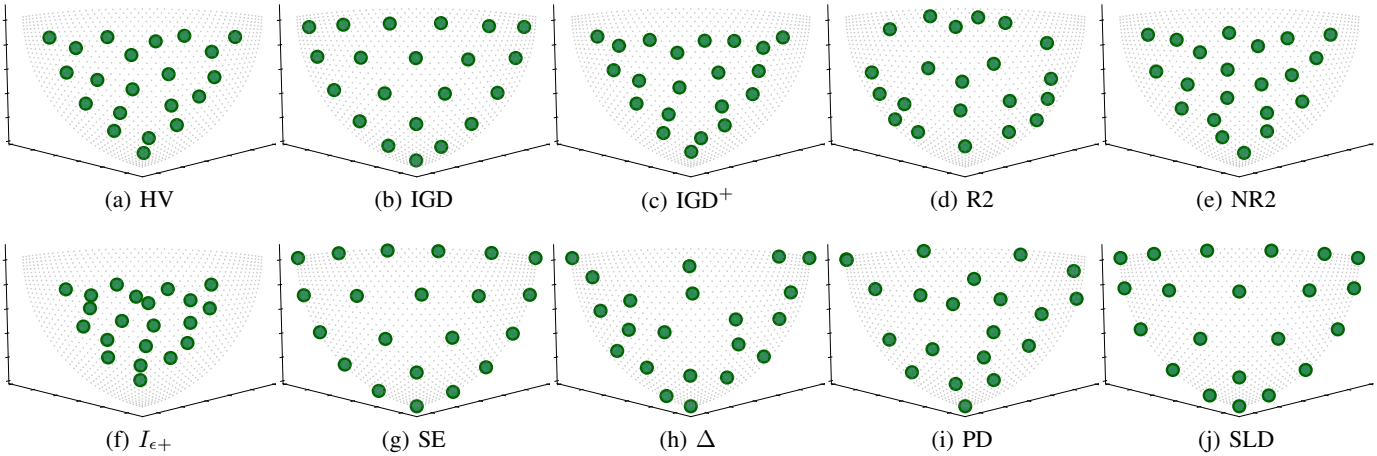

(a) HV (b) IGD (c) IGD$^+$ (d) R2 (e) NR2

(f) $I_{\epsilon+}$ (g) SE (h) Δ (i) PD (j) SLD

Fig. S.23: Approximated optimal μ-distributions with $\mu = 21$ on $F_{\text{i-convex}}$ (the inverted convex Pareto front).

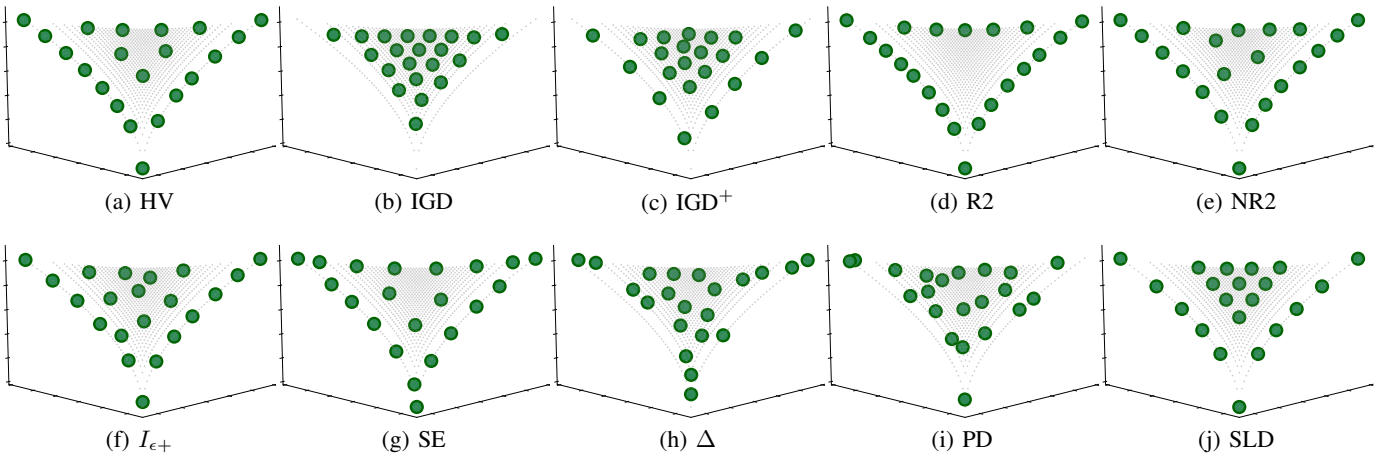

(a) HV (b) IGD (c) IGD$^+$ (d) R2 (e) NR2

(f) $I_{\epsilon+}$ (g) SE (h) Δ (i) PD (j) SLD

Fig. S.24: Approximated optimal μ-distributions with $\mu = 21$ on $F_{\text{i-concave}}$ (the inverted concave Pareto front).

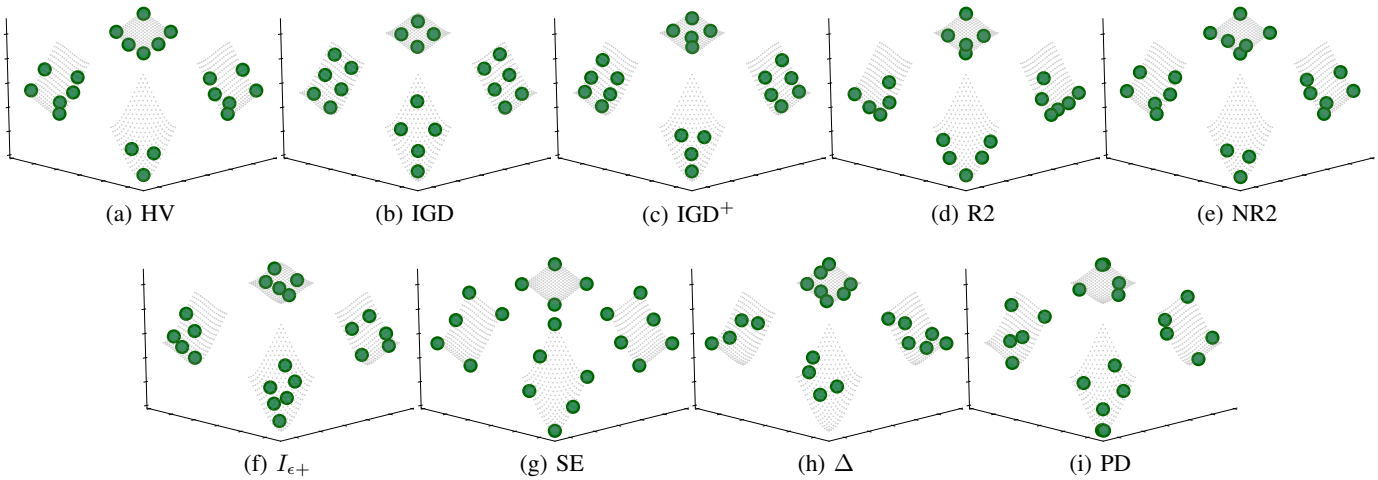

(a) HV (b) IGD (c) IGD$^+$ (d) R2 (e) NR2

(f) $I_{\epsilon+}$ (g) SE (h) Δ (i) PD

Fig. S.25: Approximated optimal μ-distributions with $\mu = 21$ on $F_{\text{disconnected}}$ (the disconnected Pareto front).

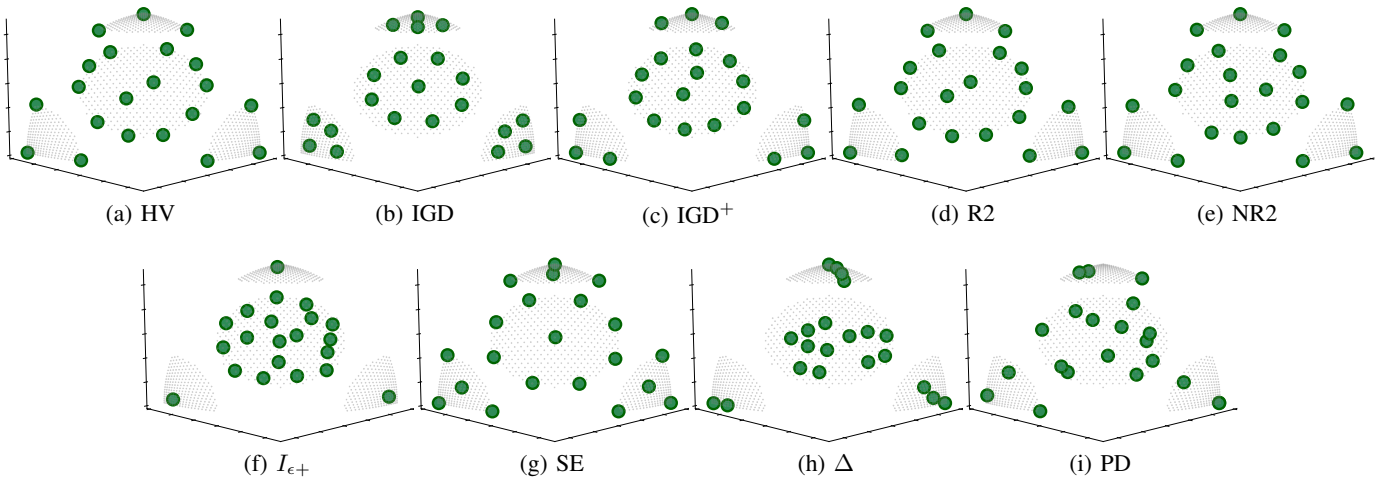

(a) HV (b) IGD (c) IGD$^+$ (d) R2 (e) NR2

(f) $I_{\epsilon+}$ (g) SE (h) Δ (i) PD

Fig. S.26: Approximated optimal μ-distributions with $\mu = 21$ on $F_{\text{c-concave}}$ (the constrained concave Pareto front).

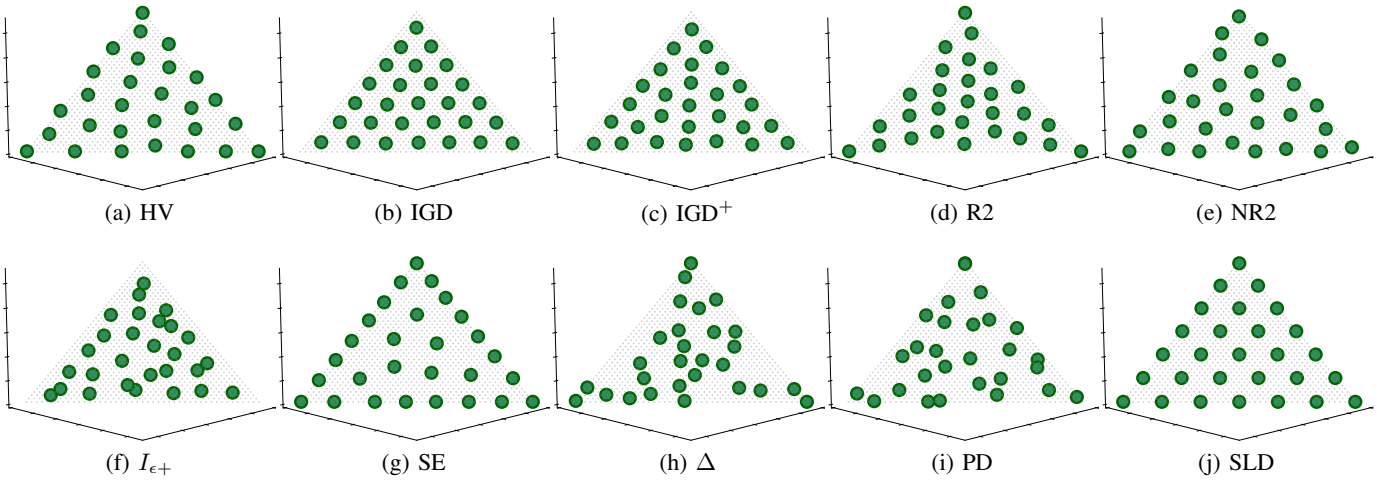

(a) HV (b) IGD (c) IGD$^+$ (d) R2 (e) NR2

(f) $I_{\epsilon+}$ (g) SE (h) Δ (i) PD (j) SLD

Fig. S.27: Approximated optimal μ-distributions with $\mu = 28$ on F_{linear} (the linear Pareto front).

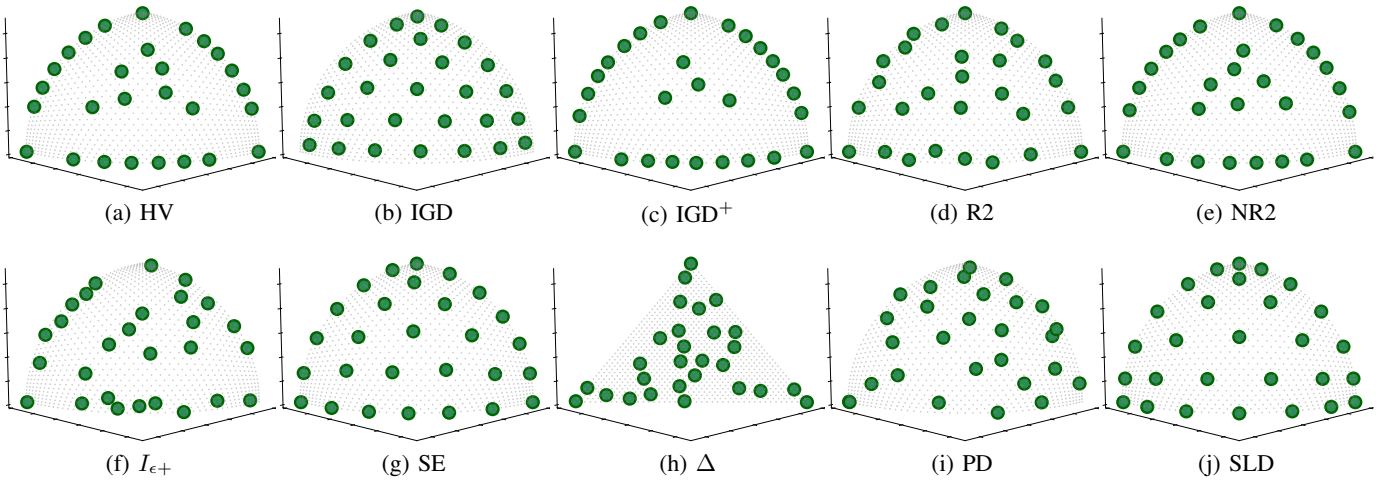

(a) HV (b) IGD (c) IGD$^+$ (d) R2 (e) NR2

(f) $I_{\epsilon+}$ (g) SE (h) Δ (i) PD (j) SLD

Fig. S.28: Approximated optimal μ-distributions with $\mu = 28$ on F_{concave} (the concave Pareto front).

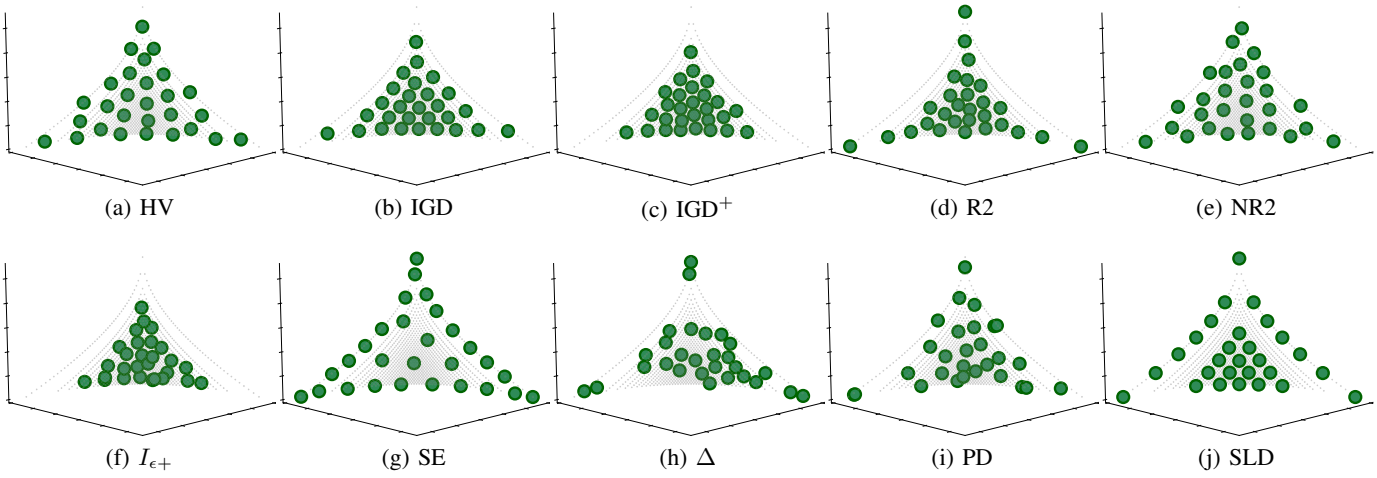

(a) HV (b) IGD (c) IGD$^+$ (d) R2 (e) NR2

(f) $I_{\epsilon+}$ (g) SE (h) Δ (i) PD (j) SLD

Fig. S.29: Approximated optimal μ-distributions with $\mu = 28$ on F_{convex} (the convex Pareto front).

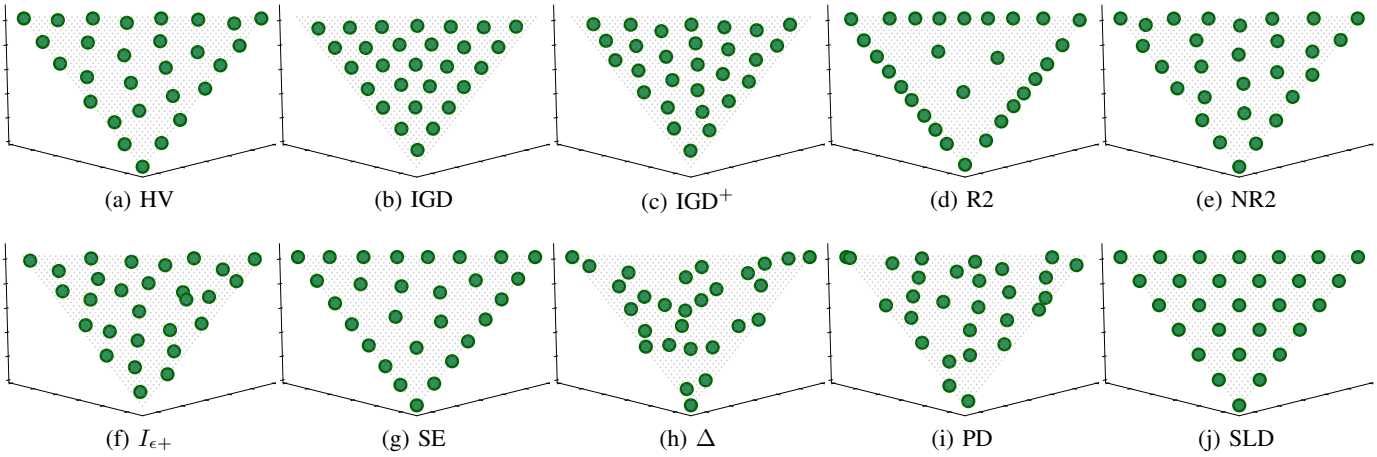

(a) HV (b) IGD (c) IGD$^+$ (d) R2 (e) NR2

(f) $I_{\epsilon+}$ (g) SE (h) Δ (i) PD (j) SLD

Fig. S.30: Approximated optimal μ-distributions with $\mu = 28$ on $F_{\text{i-linear}}$ (the inverted linear Pareto front).

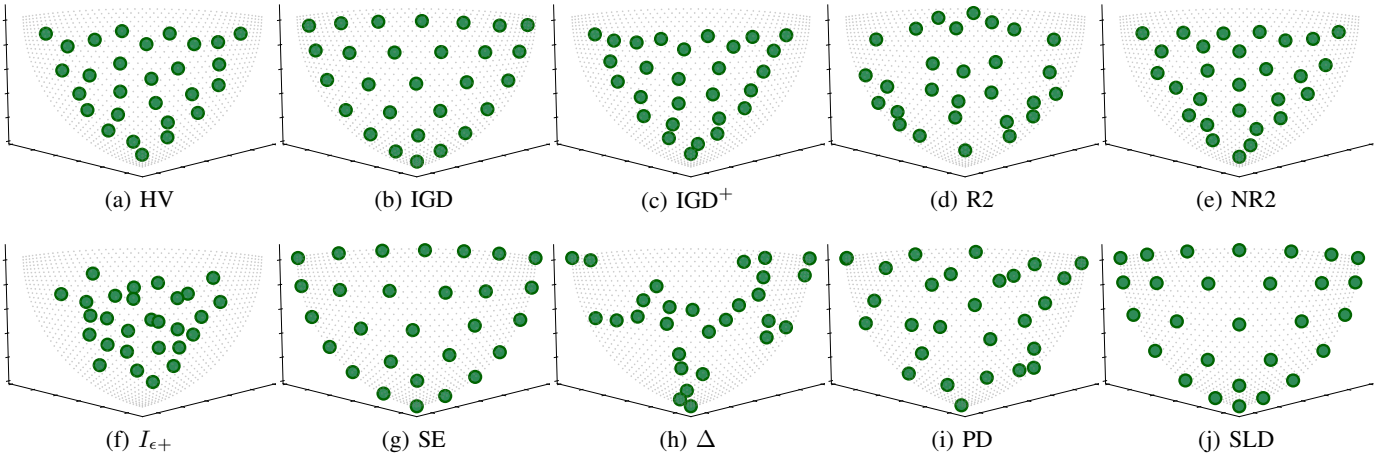

(a) HV (b) IGD (c) IGD$^+$ (d) R2 (e) NR2

(f) $I_{\epsilon+}$ (g) SE (h) Δ (i) PD (j) SLD

Fig. S.31: Approximated optimal μ-distributions with $\mu = 28$ on $F_{\text{i-convex}}$ (the inverted convex Pareto front).

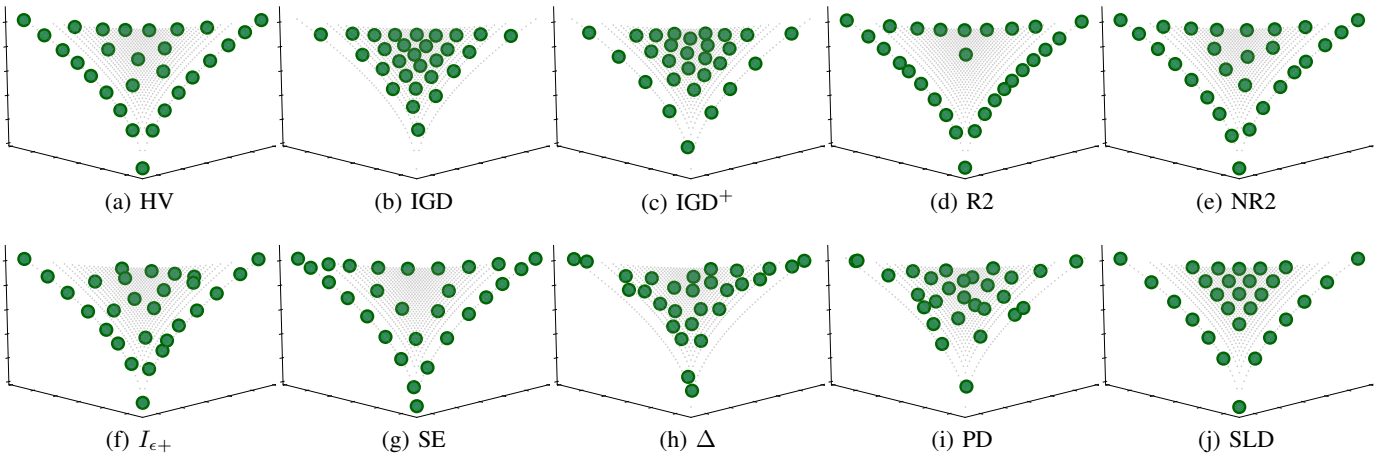

(a) HV (b) IGD (c) IGD$^+$ (d) R2 (e) NR2

(f) $I_{\epsilon+}$ (g) SE (h) Δ (i) PD (j) SLD

Fig. S.32: Approximated optimal μ-distributions with $\mu = 28$ on $F_{\text{i-concave}}$ (the inverted concave Pareto front).

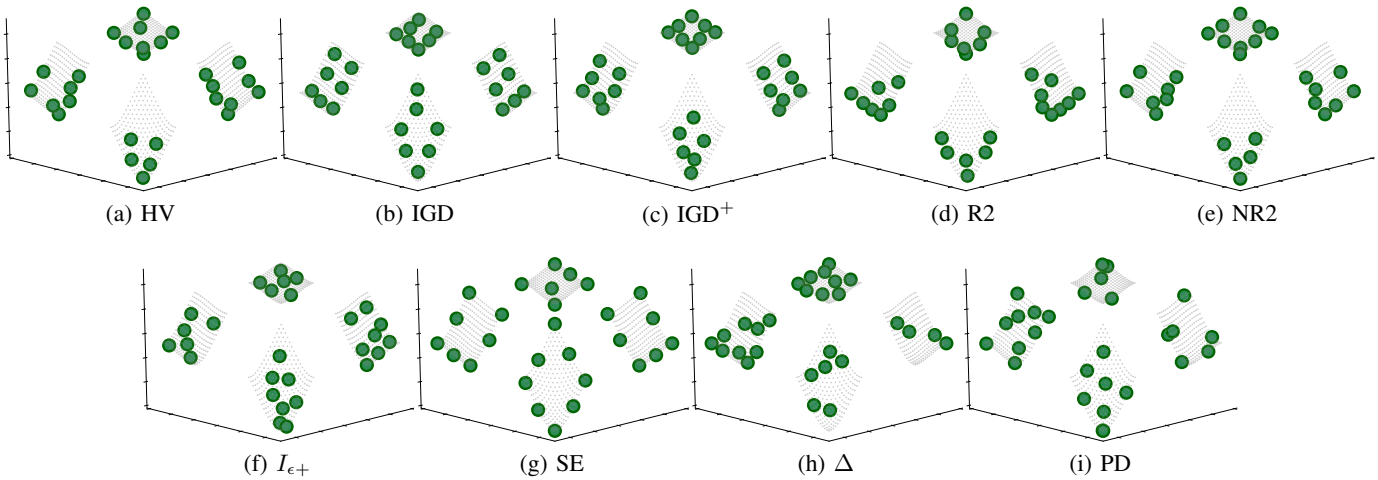

(a) HV (b) IGD (c) IGD$^+$ (d) R2 (e) NR2

(f) $I_{\epsilon+}$ (g) SE (h) Δ (i) PD

Fig. S.33: Approximated optimal μ-distributions with $\mu = 28$ on $F_{\text{disconnected}}$ (the disconnected Pareto front).

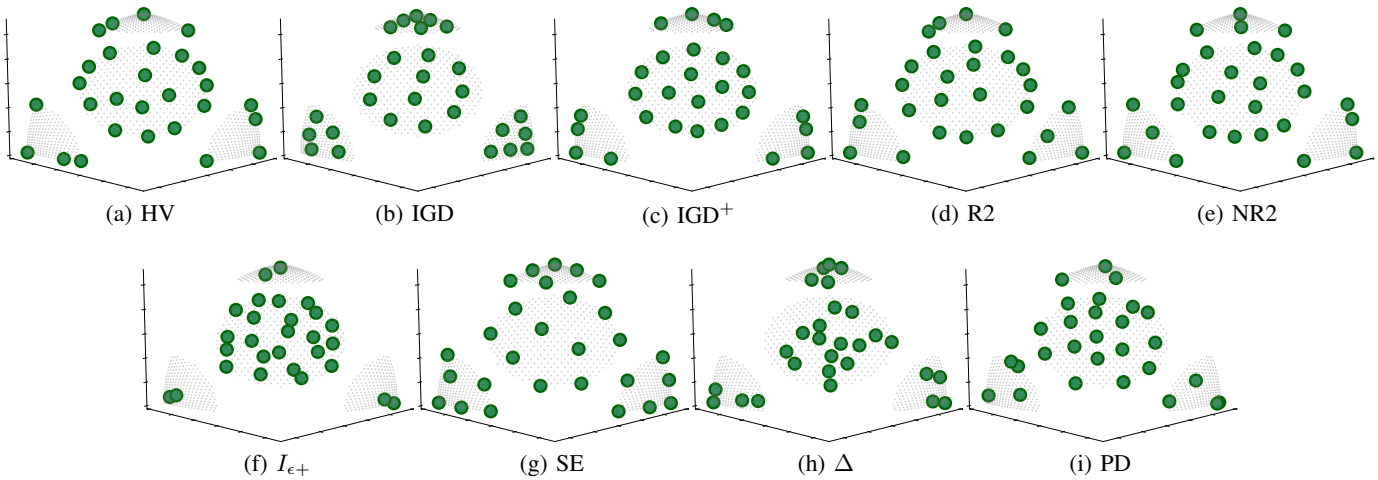

(a) HV (b) IGD (c) IGD$^+$ (d) R2 (e) NR2

(f) $I_{\epsilon+}$ (g) SE (h) Δ (i) PD

Fig. S.34: Approximated optimal μ-distributions with $\mu = 28$ on $F_{\text{c-concave}}$ (the constrained concave Pareto front).

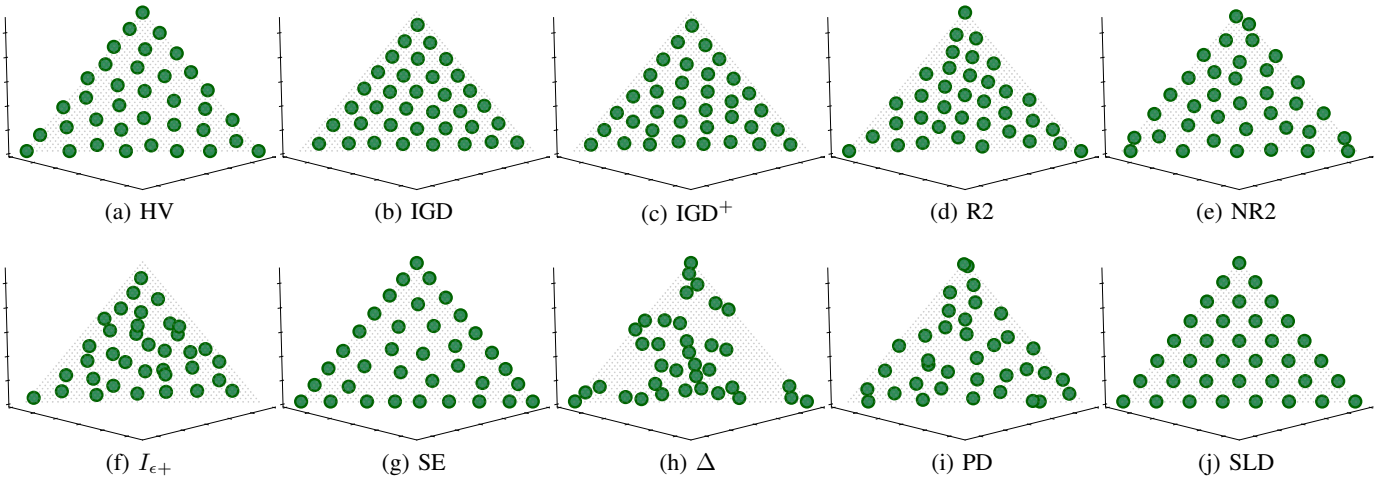

(a) HV (b) IGD (c) IGD$^+$ (d) R2 (e) NR2

(f) $I_{\epsilon+}$ (g) SE (h) Δ (i) PD (j) SLD

Fig. S.35: Approximated optimal μ-distributions with $\mu = 36$ on F_{linear} (the linear Pareto front).

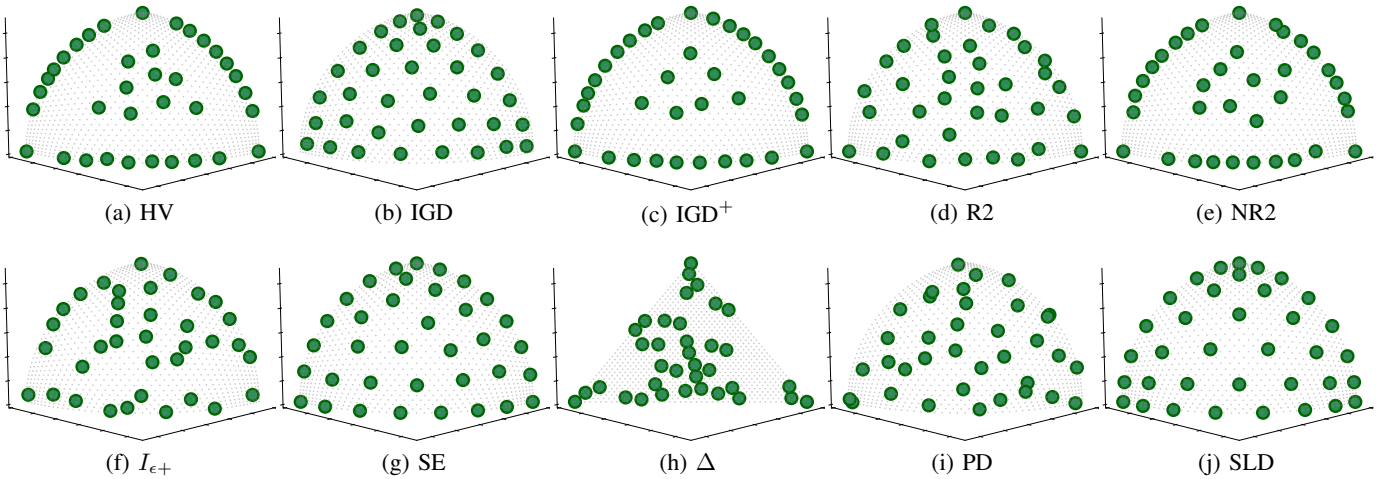

(a) HV (b) IGD (c) IGD$^+$ (d) R2 (e) NR2

(f) $I_{\epsilon+}$ (g) SE (h) Δ (i) PD (j) SLD

Fig. S.36: Approximated optimal μ-distributions with $\mu = 36$ on F_{concave} (the concave Pareto front).

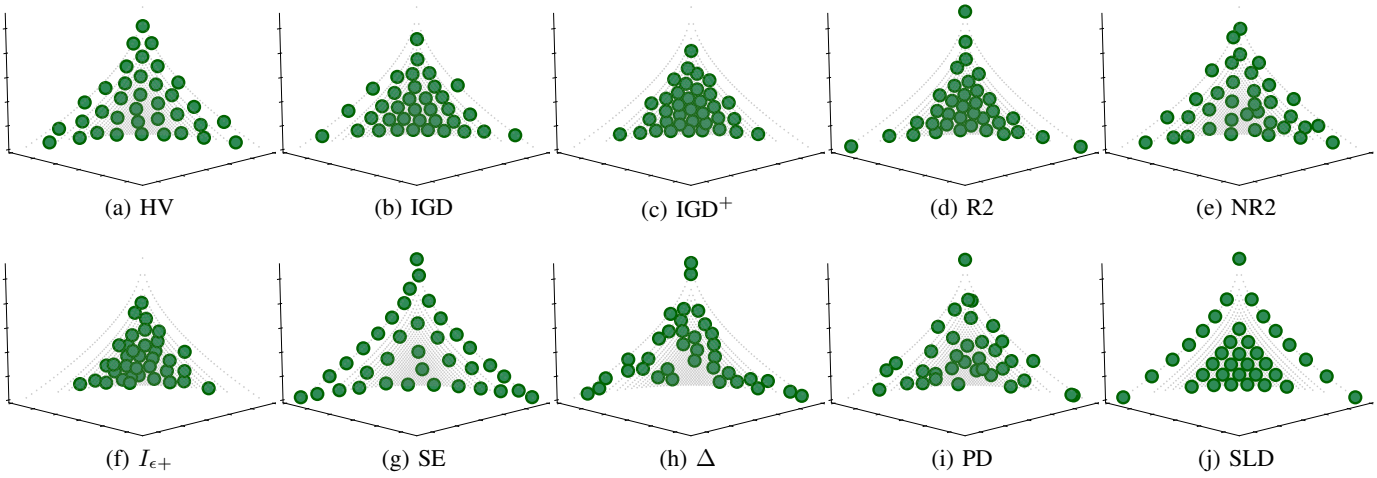

(a) HV (b) IGD (c) IGD$^+$ (d) R2 (e) NR2

(f) $I_{\epsilon+}$ (g) SE (h) Δ (i) PD (j) SLD

Fig. S.37: Approximated optimal μ-distributions with $\mu = 36$ on F_{convex} (the convex Pareto front).

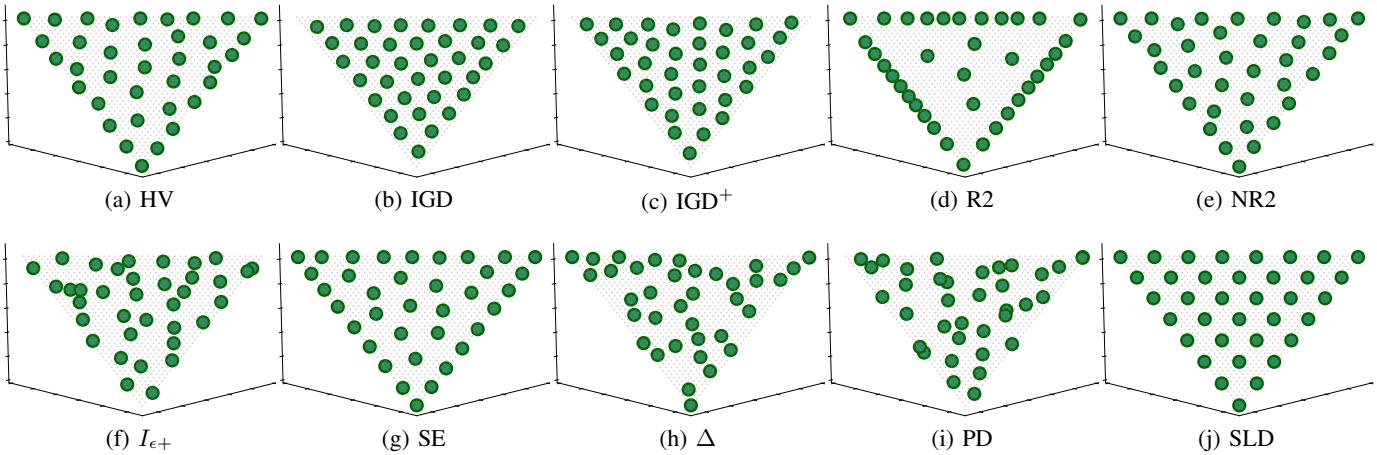

(a) HV (b) IGD (c) IGD$^+$ (d) R2 (e) NR2

(f) $I_{\epsilon+}$ (g) SE (h) Δ (i) PD (j) SLD

Fig. S.38: Approximated optimal μ-distributions with $\mu = 36$ on $F_{\text{i-linear}}$ (the inverted linear Pareto front).

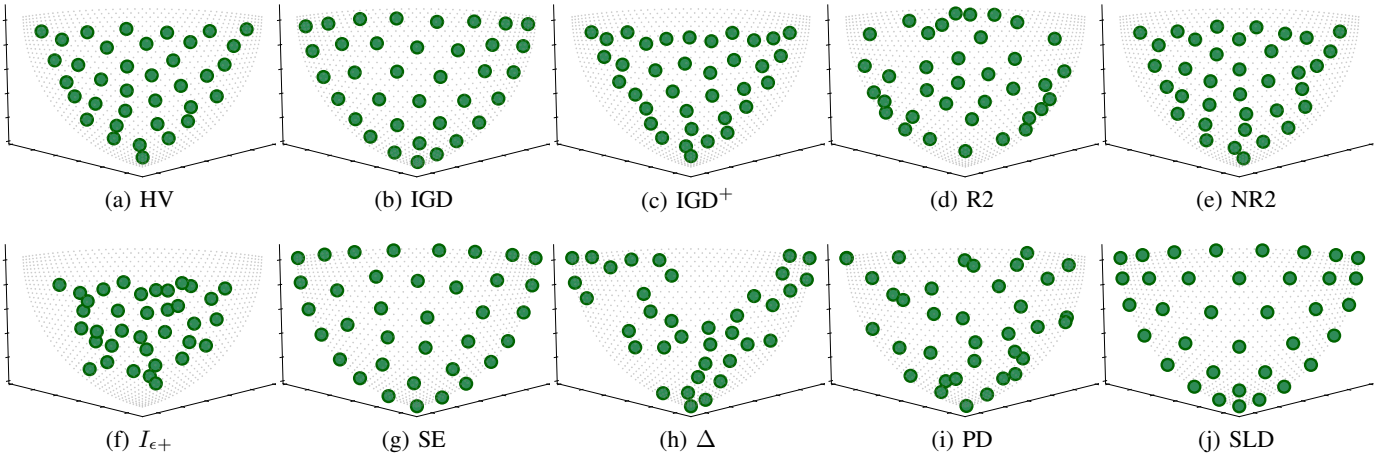

(a) HV (b) IGD (c) IGD$^+$ (d) R2 (e) NR2

(f) $I_{\epsilon+}$ (g) SE (h) Δ (i) PD (j) SLD

Fig. S.39: Approximated optimal μ-distributions with $\mu = 36$ on $F_{\text{i-convex}}$ (the inverted convex Pareto front).

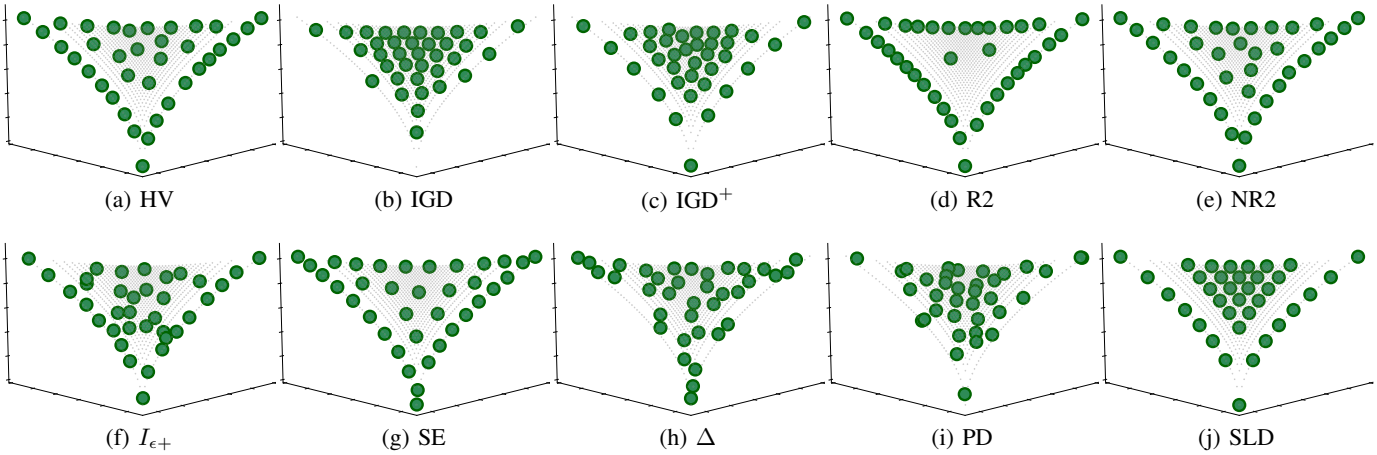

(a) HV (b) IGD (c) IGD$^+$ (d) R2 (e) NR2

(f) $I_{\epsilon+}$ (g) SE (h) Δ (i) PD (j) SLD

Fig. S.40: Approximated optimal μ-distributions with $\mu = 36$ on $F_{\text{i-concave}}$ (the inverted concave Pareto front).

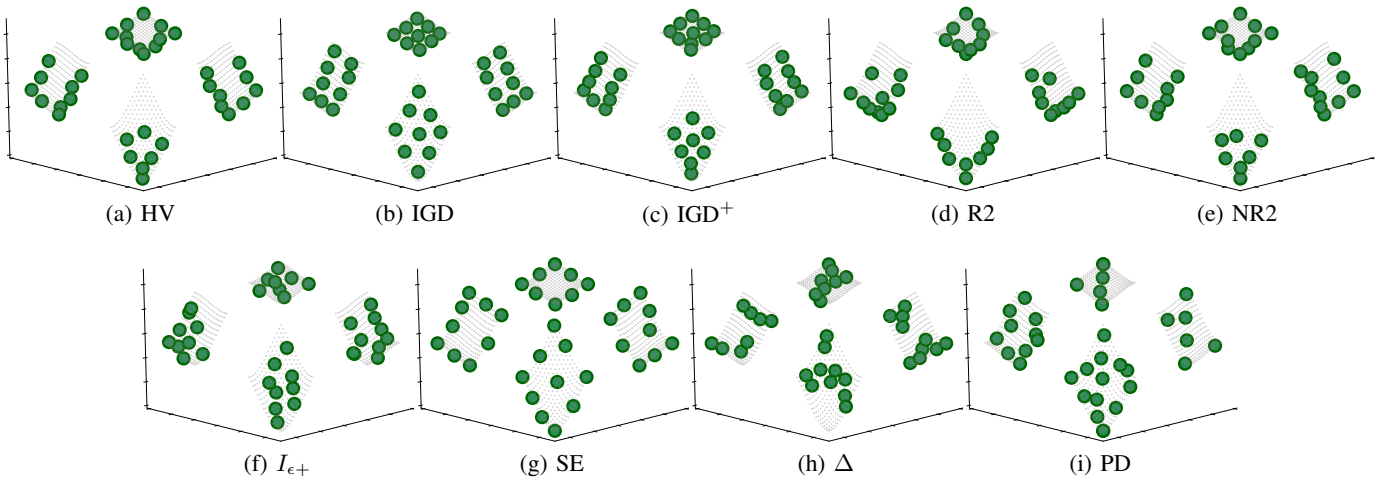

(a) HV (b) IGD (c) IGD$^+$ (d) R2 (e) NR2

(f) $I_{\epsilon+}$ (g) SE (h) Δ (i) PD

Fig. S.41: Approximated optimal μ-distributions with $\mu = 36$ on $F_{\text{disconnected}}$ (the disconnected Pareto front).

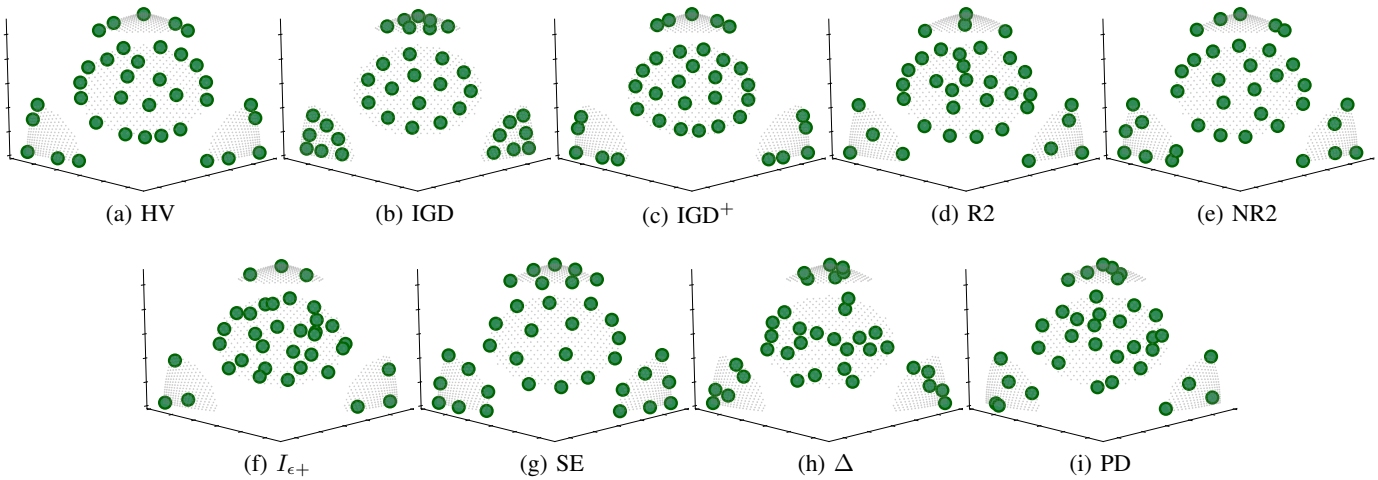

(a) HV (b) IGD (c) IGD$^+$ (d) R2 (e) NR2

(f) $I_{\epsilon+}$ (g) SE (h) Δ (i) PD

Fig. S.42: Approximated optimal μ-distributions with $\mu = 36$ on $F_{\text{c-concave}}$ (the constrained concave Pareto front).

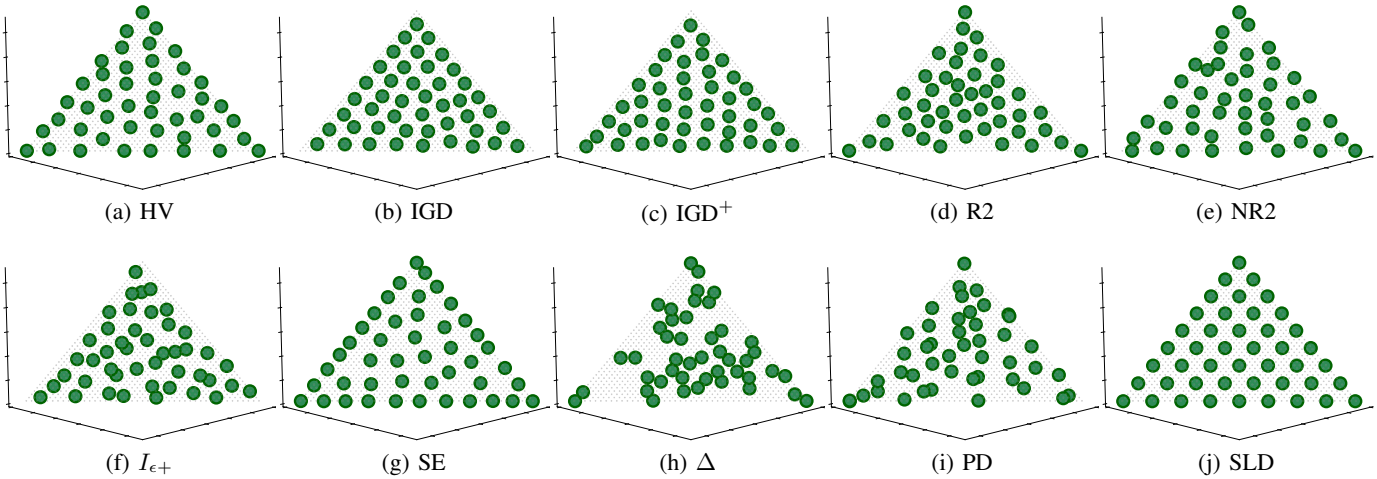

(a) HV (b) IGD (c) IGD$^+$ (d) R2 (e) NR2

(f) $I_{\epsilon+}$ (g) SE (h) Δ (i) PD (j) SLD

Fig. S.43: Approximated optimal μ-distributions with $\mu = 45$ on F_{linear} (the linear Pareto front).

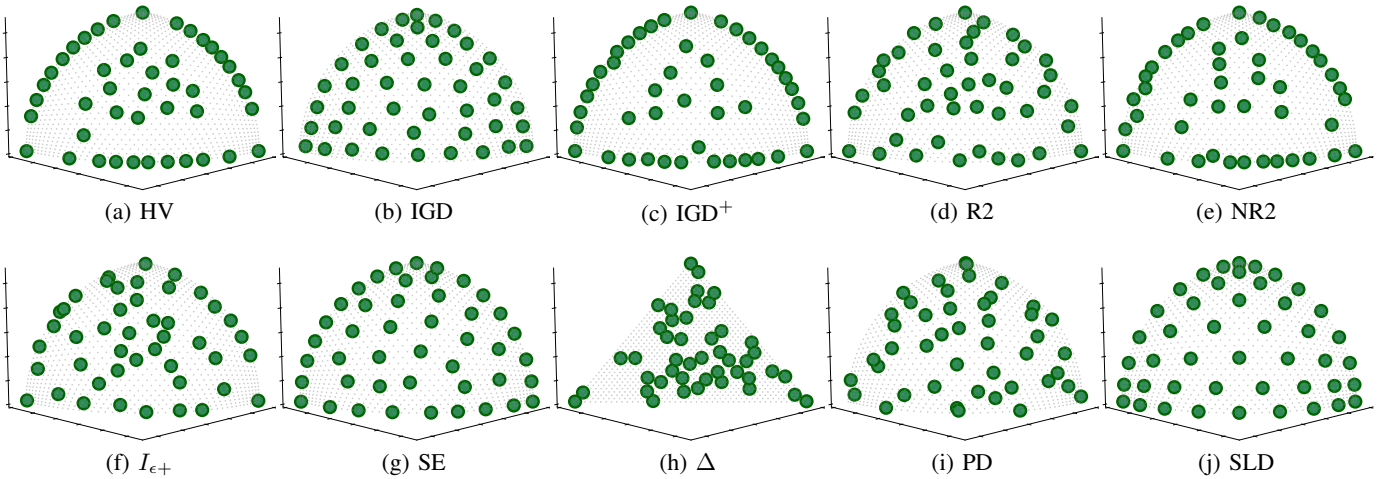

(a) HV (b) IGD (c) IGD$^+$ (d) R2 (e) NR2

(f) $I_{\epsilon+}$ (g) SE (h) Δ (i) PD (j) SLD

Fig. S.44: Approximated optimal μ-distributions with $\mu = 45$ on F_{concave} (the concave Pareto front).

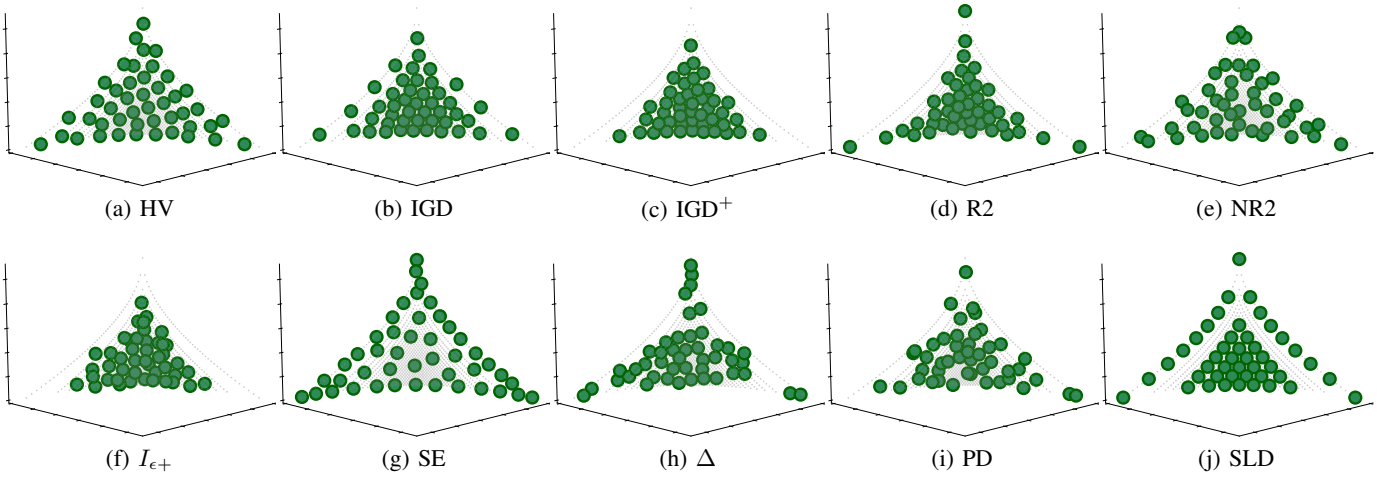

(a) HV (b) IGD (c) IGD$^+$ (d) R2 (e) NR2

(f) $I_{\epsilon+}$ (g) SE (h) Δ (i) PD (j) SLD

Fig. S.45: Approximated optimal μ-distributions with $\mu = 45$ on F_{convex} (the convex Pareto front).

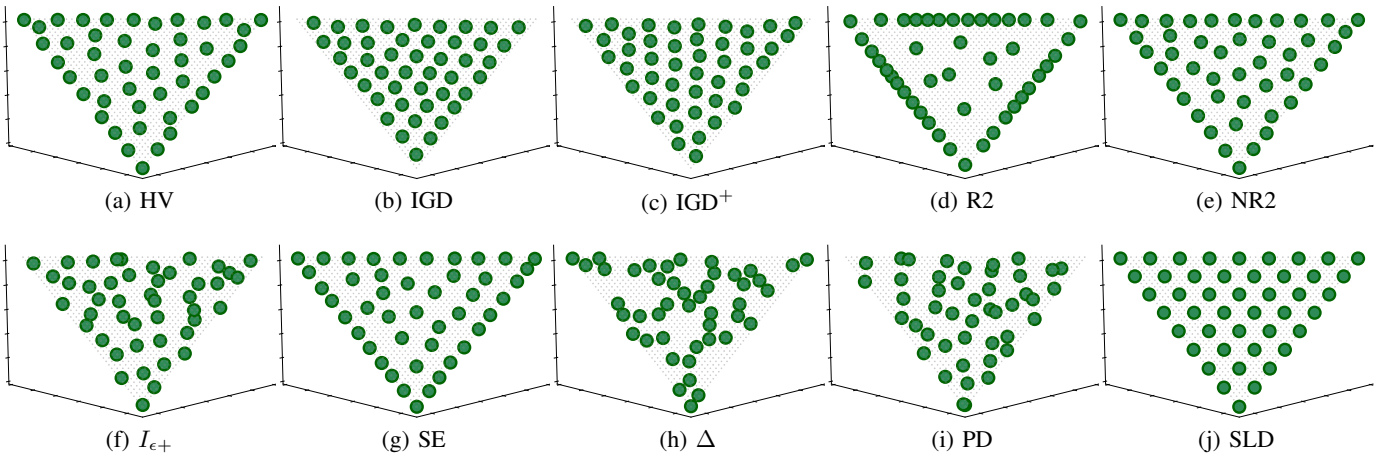

(a) HV (b) IGD (c) IGD$^+$ (d) R2 (e) NR2

(f) $I_{\epsilon+}$ (g) SE (h) Δ (i) PD (j) SLD

Fig. S.46: Approximated optimal μ-distributions with $\mu = 45$ on $F_{\text{i-linear}}$ (the inverted linear Pareto front).

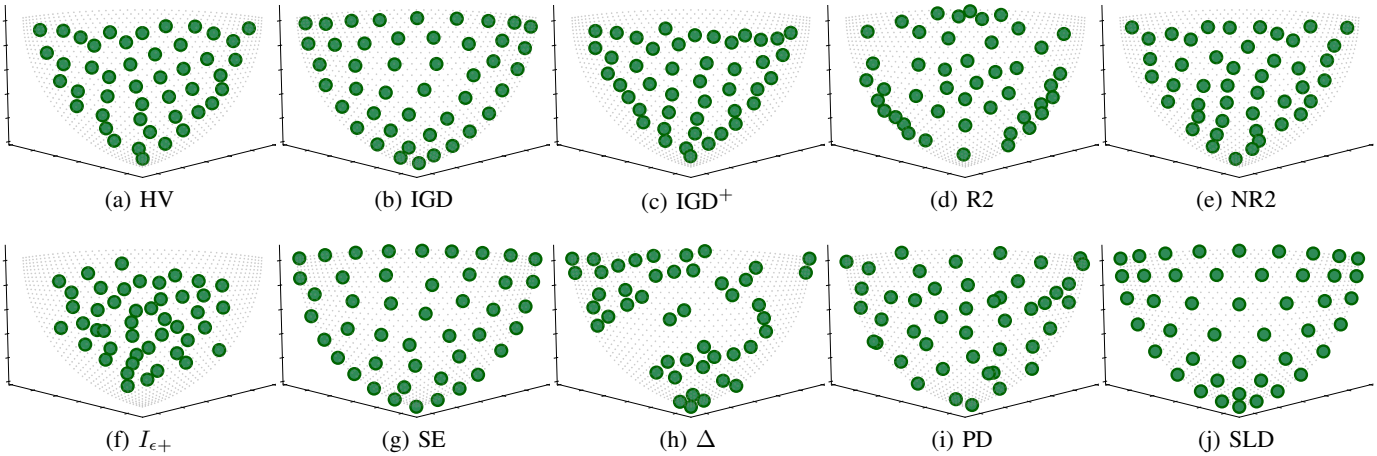

(a) HV (b) IGD (c) IGD$^+$ (d) R2 (e) NR2

(f) $I_{\epsilon+}$ (g) SE (h) Δ (i) PD (j) SLD

Fig. S.47: Approximated optimal μ-distributions with $\mu = 45$ on $F_{\text{i-convex}}$ (the inverted convex Pareto front).

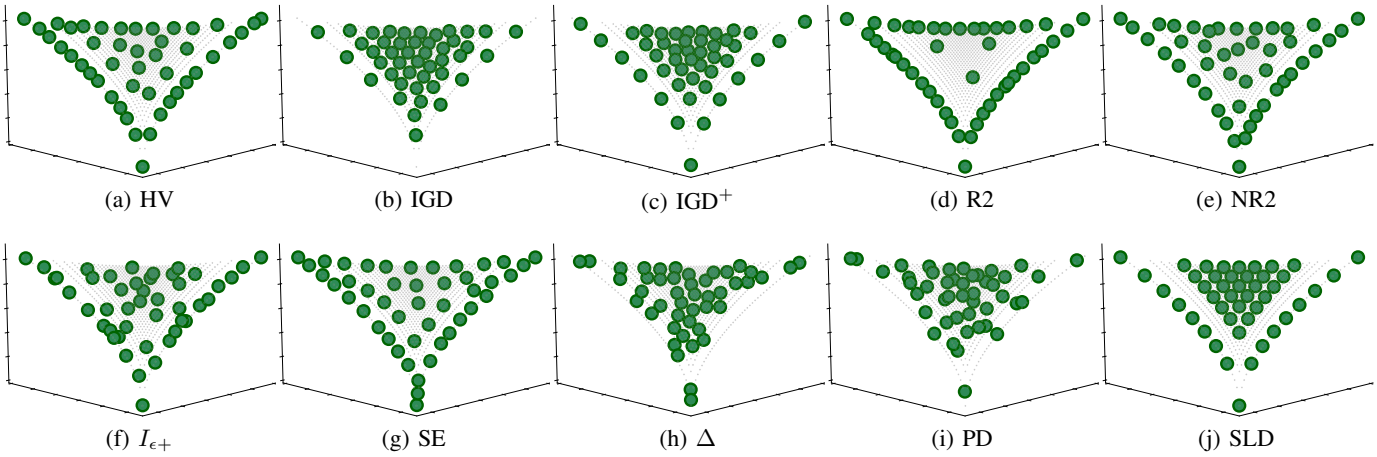

(a) HV (b) IGD (c) IGD$^+$ (d) R2 (e) NR2

(f) $I_{\epsilon+}$ (g) SE (h) Δ (i) PD (j) SLD

Fig. S.48: Approximated optimal μ-distributions with $\mu = 45$ on $F_{\text{i-concave}}$ (the inverted concave Pareto front).

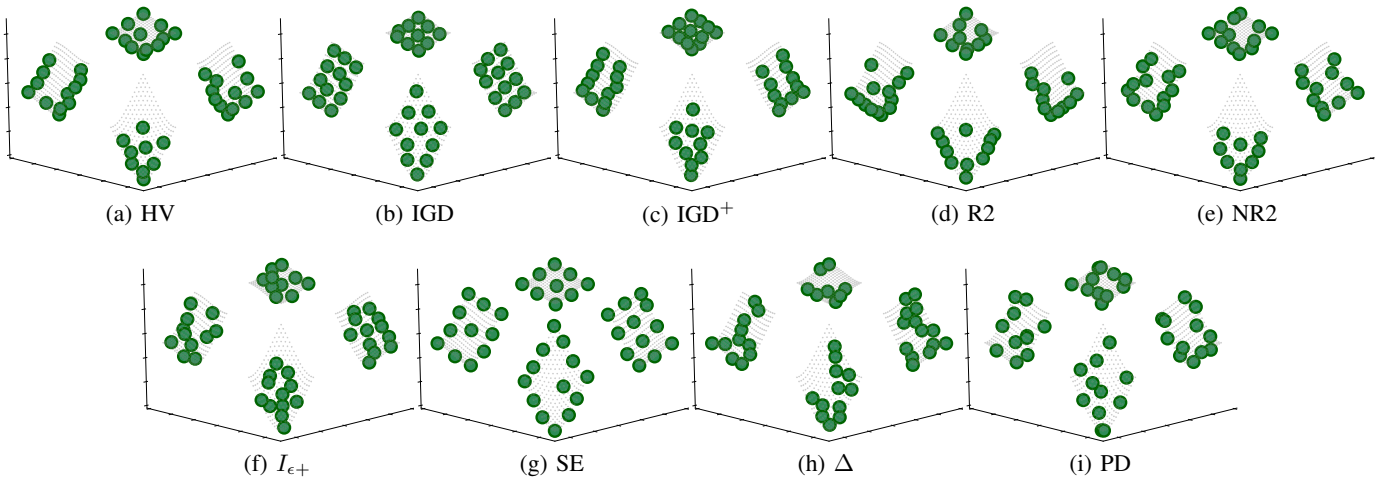

(a) HV (b) IGD (c) IGD$^+$ (d) R2 (e) NR2

(f) $I_{\epsilon+}$ (g) SE (h) Δ (i) PD

Fig. S.49: Approximated optimal μ-distributions with $\mu = 45$ on $F_{\text{disconnected}}$ (the disconnected Pareto front).

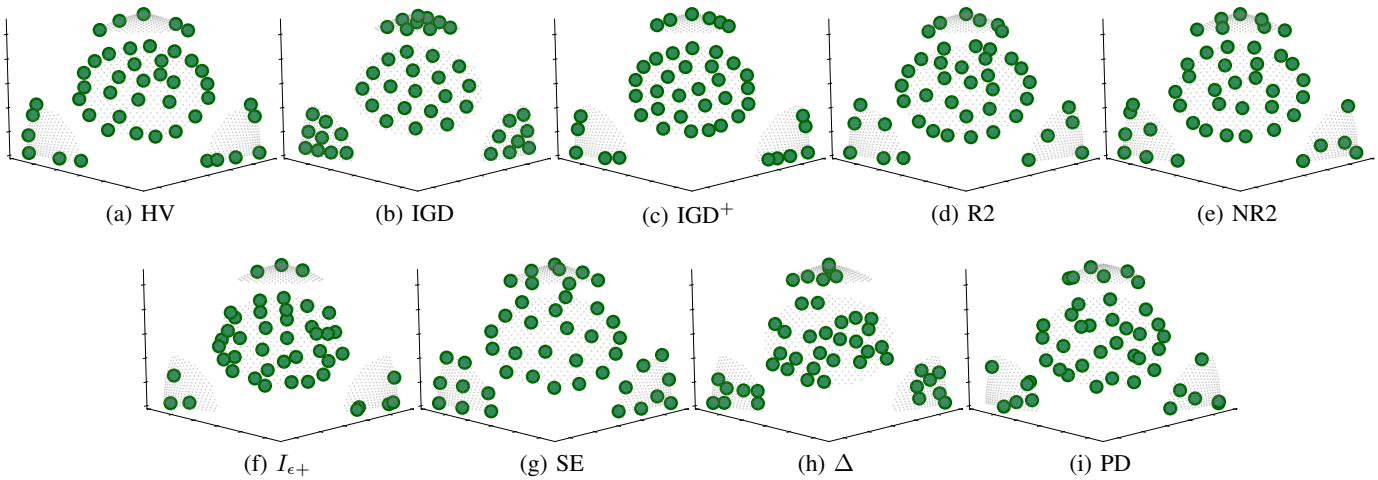

(a) HV (b) IGD (c) IGD$^+$ (d) R2 (e) NR2

(f) $I_{\epsilon+}$ (g) SE (h) Δ (i) PD

Fig. S.50: Approximated optimal μ-distributions with $\mu = 45$ on $F_{\text{c-concave}}$ (the constrained concave Pareto front).

REFERENCES

[S.1] T. Okabe, Y. Jin, and B. Sendhoff, "A Critical Survey of Performance Indices for Multi-Objective Optimisation," in *IEEE CEC*, 2002, pp. 878–885.

[S.2] Y. Tian, X. Xiang, X. Zhang, R. Cheng, and Y. Jin, "Sampling Reference Points on the Pareto Fronts of Benchmark Multi-Objective Optimization Problems," in *IEEE CEC*, 2018, pp. 1–6.

[S.3] I. Das and J. E. Dennis, "Normal-Boundary Intersection: A New Method for Generating the Pareto Surface in Nonlinear Multicriteria Optimization Problems," *SIAM J. Optimiz*, vol. 8, no. 3, pp. 631–657, 1998.

[S.4] A. Auger, J. Bader, D. Brockhoff, and E. Zitzler, "Theory of the hypervolume indicator: optimal μ-distributions and the choice of the reference point," in *FOGA*, 2009, pp. 87–102.

[S.5] M. Li, S. Yang, and X. Liu, "Diversity Comparison of Pareto Front Approximations in Many-Objective Optimization," *IEEE Trans. Cyber.*, vol. 44, no. 12, pp. 2568–2584, 2014.

TABLE S.2: Rankings of the nine approximated optimal μ-distributions ($\boldsymbol{A}_{\mathrm{HV}}$, ..., $\boldsymbol{A}_{\mathrm{PD}}$) and $\boldsymbol{A}_{\mathrm{SLD}}$ by each quality indicator on F_{linear}.

	$\boldsymbol{A}_{\mathrm{HV}}$	$\boldsymbol{A}_{\mathrm{IGD}}$	$\boldsymbol{A}_{\mathrm{IGD}^+}$	$\boldsymbol{A}_{\mathrm{R2}}$	$\boldsymbol{A}_{\mathrm{NR2}}$	$\boldsymbol{A}_{I_{\epsilon+}}$	$\boldsymbol{A}_{\mathrm{SE}}$	$\boldsymbol{A}_{\Delta}$	$\boldsymbol{A}_{\mathrm{PD}}$	$\boldsymbol{A}_{\mathrm{SLD}}$
HV	1	8	9	6	2	10	4	7	5	3
IGD	6	1	2	4	5	3	10	9	7	8
IGD$^+$	6	1	2	4	5	3	10	9	7	8
R2	3	8	9	1	5	10	6	4	7	2
NR2	2	8	9	6	1	10	4	7	5	3
$I_{\epsilon+}$	5	2	3	6	4	1	9	10	8	7
SE	3	7	8	5	4	9	1	6	10	2
Δ	3	6	7	2	4	9	5	1	10	8
PD	6	8	7	2	5	4	9	3	1	10
Avg.	3.5	4.9	5.6	3.6	3.5	5.9	5.8	5.6	6.0	5.1

TABLE S.3: Rankings of the nine approximated optimal μ-distributions ($\boldsymbol{A}_{\mathrm{HV}}$, ..., $\boldsymbol{A}_{\mathrm{PD}}$) and $\boldsymbol{A}_{\mathrm{SLD}}$ by each quality indicator on F_{convex}.

	$\boldsymbol{A}_{\mathrm{HV}}$	$\boldsymbol{A}_{\mathrm{IGD}}$	$\boldsymbol{A}_{\mathrm{IGD}^+}$	$\boldsymbol{A}_{\mathrm{R2}}$	$\boldsymbol{A}_{\mathrm{NR2}}$	$\boldsymbol{A}_{I_{\epsilon+}}$	$\boldsymbol{A}_{\mathrm{SE}}$	$\boldsymbol{A}_{\Delta}$	$\boldsymbol{A}_{\mathrm{PD}}$	$\boldsymbol{A}_{\mathrm{SLD}}$
HV	1	8	9	6	2	10	4	7	3	5
IGD	7	1	2	3	6	4	10	8	5	9
IGD$^+$	7	3	1	4	6	2	10	8	5	9
R2	2	7	8	1	3	10	9	5	4	6
NR2	2	8	9	6	1	10	4	7	3	5
$I_{\epsilon+}$	5	3	2	4	7	1	10	8	6	9
SE	2	8	9	6	4	10	1	5	7	3
Δ	3	5	9	6	4	10	2	1	7	8
PD	4	8	6	2	3	7	9	5	1	10
Avg.	3.3	5.1	5.5	3.8	3.6	6.4	5.9	5.4	4.1	6.4

TABLE S.4: Rankings of the nine approximated optimal μ-distributions ($\boldsymbol{A}_{\mathrm{HV}}$, ..., $\boldsymbol{A}_{\mathrm{PD}}$) and $\boldsymbol{A}_{\mathrm{SLD}}$ by each quality indicator on $F_{\mathrm{i\text{-}linear}}$.

	$\boldsymbol{A}_{\mathrm{HV}}$	$\boldsymbol{A}_{\mathrm{IGD}}$	$\boldsymbol{A}_{\mathrm{IGD}^+}$	$\boldsymbol{A}_{\mathrm{R2}}$	$\boldsymbol{A}_{\mathrm{NR2}}$	$\boldsymbol{A}_{I_{\epsilon+}}$	$\boldsymbol{A}_{\mathrm{SE}}$	$\boldsymbol{A}_{\Delta}$	$\boldsymbol{A}_{\mathrm{PD}}$	$\boldsymbol{A}_{\mathrm{SLD}}$
HV	1	8	7	9	2	5	4	10	6	3
IGD	4	1	2	10	5	3	9	8	6	7
IGD$^+$	4	2	1	10	5	3	9	8	6	7
R2	5	8	9	1	4	7	2	10	6	3
NR2	2	8	7	9	1	6	4	10	5	3
$I_{\epsilon+}$	2	5	6	10	4	1	8	9	7	3
SE	4	7	8	5	3	6	1	9	10	2
Δ	3	5	7	8	2	9	4	1	10	6
PD	4	7	2	8	5	3	9	6	1	10
Avg.	2.9	5.1	4.9	7.0	3.1	4.3	5.0	7.1	5.7	4.4

TABLE S.5: Rankings of the nine approximated optimal μ-distributions ($\boldsymbol{A}_{\mathrm{HV}}$, ..., $\boldsymbol{A}_{\mathrm{PD}}$) and $\boldsymbol{A}_{\mathrm{SLD}}$ by each quality indicator on $F_{\mathrm{i\text{-}concave}}$.

	$\boldsymbol{A}_{\mathrm{HV}}$	$\boldsymbol{A}_{\mathrm{IGD}}$	$\boldsymbol{A}_{\mathrm{IGD}^+}$	$\boldsymbol{A}_{\mathrm{R2}}$	$\boldsymbol{A}_{\mathrm{NR2}}$	$\boldsymbol{A}_{I_{\epsilon+}}$	$\boldsymbol{A}_{\mathrm{SE}}$	$\boldsymbol{A}_{\Delta}$	$\boldsymbol{A}_{\mathrm{PD}}$	$\boldsymbol{A}_{\mathrm{SLD}}$
HV	1	10	7	3	2	6	5	9	8	4
IGD	7	1	2	10	8	5	9	3	4	6
IGD$^+$	5	4	1	10	7	3	8	9	6	2
R2	2	10	7	1	3	6	4	8	9	5
NR2	1	10	7	3	2	6	5	9	8	4
$I_{\epsilon+}$	2	10	9	6	3	1	5	7	8	4
SE	3	10	9	4	2	5	1	7	8	6
Δ	4	7	10	5	3	6	2	1	9	8
PD	7	3	4	9	8	5	6	2	1	10
Avg.	3.2	6.5	5.6	5.1	3.8	4.3	4.5	5.5	6.1	4.9

TABLE S.6: Rankings of the nine approximated optimal μ-distributions ($\boldsymbol{A}_{\mathrm{HV}}$, ..., $\boldsymbol{A}_{\mathrm{PD}}$) and $\boldsymbol{A}_{\mathrm{SLD}}$ by each quality indicator on $F_{\text{i-convex}}$.

	$\boldsymbol{A}_{\mathrm{HV}}$	$\boldsymbol{A}_{\mathrm{IGD}}$	$\boldsymbol{A}_{\mathrm{IGD}^+}$	$\boldsymbol{A}_{\mathrm{R2}}$	$\boldsymbol{A}_{\mathrm{NR2}}$	$\boldsymbol{A}_{I_{\epsilon+}}$	$\boldsymbol{A}_{\mathrm{SE}}$	$\boldsymbol{A}_{\Delta}$	$\boldsymbol{A}_{\mathrm{PD}}$	$\boldsymbol{A}_{\mathrm{SLD}}$
HV	1	5	3	6	2	4	9	8	7	10
IGD	7	1	8	9	6	10	5	3	2	4
IGD^+	2	5	1	6	3	4	9	8	7	10
R2	3	5	4	1	2	8	7	10	6	9
NR2	2	4	3	6	1	5	9	8	7	10
$I_{\epsilon+}$	2	6	4	5	3	1	9	8	7	10
SE	7	3	8	5	6	9	1	4	10	2
Δ	4	3	6	9	5	10	2	1	8	7
PD	4	7	6	3	2	8	9	5	1	10
Avg.	3.2	3.9	4.3	5.0	3.0	5.9	6.0	5.5	5.5	7.2

TABLE S.7: Kendall rank correlation τ values of the nine quality indicator on F_{linear}.

	HV	IGD	IGD^+	R2	NR2	$I_{\epsilon+}$	SE	Δ	PD
HV	1.00	-0.33	-0.33	0.56	0.96	-0.24	0.56	0.24	-0.11
IGD	-0.33	1.00	1.00	-0.24	-0.29	0.73	-0.42	-0.11	-0.02
IGD^+	-0.33	1.00	1.00	-0.24	-0.29	0.73	-0.42	-0.11	-0.02
R2	0.56	-0.24	-0.24	1.00	0.51	-0.42	0.47	0.51	-0.02
NR2	0.96	-0.29	-0.29	0.51	1.00	-0.20	0.51	0.20	-0.07
$I_{\epsilon+}$	-0.24	0.73	0.73	-0.42	-0.20	1.00	-0.33	-0.29	-0.11
SE	0.56	-0.42	-0.42	0.47	0.51	-0.33	1.00	0.33	-0.47
Δ	0.24	-0.11	-0.11	0.51	0.20	-0.29	0.33	1.00	0.11
PD	-0.11	-0.02	-0.02	-0.02	-0.07	-0.11	-0.47	0.11	1.00

TABLE S.8: Kendall rank correlation τ values of the nine quality indicator on F_{convex}.

	HV	IGD	IGD^+	R2	NR2	$I_{\epsilon+}$	SE	Δ	PD
HV	1.00	-0.38	-0.51	0.56	0.96	-0.47	0.64	0.38	0.24
IGD	-0.38	1.00	0.87	0.07	-0.33	0.73	-0.64	-0.38	0.20
IGD^+	-0.51	0.87	1.00	-0.07	-0.47	0.87	-0.78	-0.51	0.24
R2	0.56	0.07	-0.07	1.00	0.51	-0.02	0.29	0.29	0.51
NR2	0.96	-0.33	-0.47	0.51	1.00	-0.51	0.60	0.33	0.29
$I_{\epsilon+}$	-0.47	0.73	0.87	-0.02	-0.51	1.00	-0.73	-0.47	0.11
SE	0.64	-0.64	-0.78	0.29	0.60	-0.73	1.00	0.56	-0.11
Δ	0.38	-0.38	-0.51	0.29	0.33	-0.47	0.56	1.00	-0.02
PD	0.24	0.20	0.24	0.51	0.29	0.11	-0.11	-0.02	1.00

TABLE S.9: Kendall rank correlation τ values of the nine quality indicator on $F_{\text{i-linear}}$.

	HV	IGD	IGD^+	R2	NR2	$I_{\epsilon+}$	SE	Δ	PD
HV	1.00	0.07	0.11	0.29	0.91	0.47	0.38	0.16	-0.02
IGD	0.07	1.00	0.96	-0.56	-0.02	0.51	-0.29	-0.07	0.38
IGD^+	0.11	0.96	1.00	-0.60	0.02	0.47	-0.33	-0.11	0.42
R2	0.29	-0.56	-0.60	1.00	0.38	-0.07	0.64	-0.11	-0.38
NR2	0.91	-0.02	0.02	0.38	1.00	0.38	0.38	0.16	-0.02
$I_{\epsilon+}$	0.47	0.51	0.47	-0.07	0.38	1.00	0.20	-0.02	0.16
SE	0.38	-0.29	-0.33	0.64	0.38	0.20	1.00	0.24	-0.56
Δ	0.16	-0.07	-0.11	-0.11	0.16	-0.02	0.24	1.00	-0.24
PD	-0.02	0.38	0.42	-0.38	-0.02	0.16	-0.56	-0.24	1.00

TABLE S.10: Kendall rank correlation τ values of the nine quality indicator on $F_{\text{i-concave}}$.

	HV	IGD	IGD^+	R2	NR2	$I_{\epsilon+}$	SE	Δ	PD
HV	1.00	-0.64	-0.07	0.82	1.00	0.56	0.60	0.20	-0.60
IGD	-0.64	1.00	0.42	-0.73	-0.64	-0.38	-0.78	-0.38	0.51
IGD^+	-0.07	0.42	1.00	-0.24	-0.07	0.02	-0.38	-0.60	0.02
R2	0.82	-0.73	-0.24	1.00	0.82	0.47	0.60	0.20	-0.69
NR2	1.00	-0.64	-0.07	0.82	1.00	0.56	0.60	0.20	-0.60
$I_{\epsilon+}$	0.56	-0.38	0.02	0.47	0.56	1.00	0.60	0.20	-0.33
SE	0.60	-0.78	-0.38	0.60	0.60	0.60	1.00	0.60	-0.38
Δ	0.20	-0.38	-0.60	0.20	0.20	0.20	0.60	1.00	-0.07
PD	-0.60	0.51	0.02	-0.69	-0.60	-0.33	-0.38	-0.07	1.00

TABLE S.11: Kendall rank correlation τ values of the nine quality indicator on $F_{\text{i-convex}}$.

	HV	IGD	IGD$^+$	R2	NR2	$I_{\epsilon+}$	SE	Δ	PD
HV	1.00	-0.20	0.91	0.51	0.91	0.82	-0.38	-0.07	0.33
IGD	-0.20	1.00	-0.29	-0.24	-0.11	-0.38	0.29	0.42	0.02
IGD$^+$	0.91	-0.29	1.00	0.42	0.82	0.73	-0.47	-0.16	0.24
R2	0.51	-0.24	0.42	1.00	0.60	0.42	-0.07	-0.20	0.47
NR2	0.91	-0.11	0.82	0.60	1.00	0.73	-0.29	-0.07	0.42
$I_{\epsilon+}$	0.82	-0.38	0.73	0.42	0.73	1.00	-0.56	-0.24	0.24
SE	-0.38	0.29	-0.47	-0.07	-0.29	-0.56	1.00	0.42	-0.42
Δ	-0.07	0.42	-0.16	-0.20	-0.07	-0.24	0.42	1.00	-0.11
PD	0.33	0.02	0.24	0.47	0.42	0.24	-0.42	-0.11	1.00

TABLE S.12: Rankings of the nine approximated optimal μ-distributions ($\boldsymbol{A}_{\text{HV}}$, ..., $\boldsymbol{A}_{\text{PD}}$) by each quality indicator on F_{linear} with $m = 5$.

	$\boldsymbol{A}_{\text{HV}}$	$\boldsymbol{A}_{\text{IGD}}$	$\boldsymbol{A}_{\text{IGD+}}$	$\boldsymbol{A}_{\text{R2}}$	$\boldsymbol{A}_{\text{NR2}}$	$\boldsymbol{A}_{I_{\epsilon+}}$	$\boldsymbol{A}_{\text{SE}}$	$\boldsymbol{A}_{\Delta}$	$\boldsymbol{A}_{\text{PD}}$
HV	1	8	9	6	2	7	3	4	5
IGD	7	1	2	3	8	5	9	6	4
IGDP	7	2	1	3	8	4	9	6	5
R2	5	7	8	1	4	9	2	3	6
NR2	2	8	9	5	1	7	3	4	6
$I_{\epsilon+}$	8	2	3	4	6	1	9	7	5
SE	2	7	8	5	4	9	1	3	6
Δ	3	4	5	6	7	9	2	1	8
PD	7	5	6	3	8	4	9	2	1
Avg.	4.7	4.9	5.7	4.0	5.3	6.1	5.2	4.0	5.1

TABLE S.13: Rankings of the nine approximated optimal μ-distributions ($\boldsymbol{A}_{\text{HV}}$, ..., $\boldsymbol{A}_{\text{PD}}$) by each quality indicator on F_{concave} with $m = 5$.

	$\boldsymbol{A}_{\text{HV}}$	$\boldsymbol{A}_{\text{IGD}}$	$\boldsymbol{A}_{\text{IGD+}}$	$\boldsymbol{A}_{\text{R2}}$	$\boldsymbol{A}_{\text{NR2}}$	$\boldsymbol{A}_{I_{\epsilon+}}$	$\boldsymbol{A}_{\text{SE}}$	$\boldsymbol{A}_{\Delta}$	$\boldsymbol{A}_{\text{PD}}$
HV	1	9	2	5	4	8	3	6	7
IGD	9	1	8	3	7	2	6	5	4
IGD$^+$	2	7	1	4	3	8	5	6	9
R2	2	9	4	1	3	8	5	6	7
NR2	3	9	2	5	1	8	4	6	7
$I_{\epsilon+}$	3	2	4	5	6	1	7	9	8
SE	7	6	3	4	2	8	1	5	9
Δ	8	4	6	5	3	9	2	1	7
PD	9	4	8	5	7	3	6	2	1
Avg.	4.9	5.7	4.2	4.1	4.0	6.1	4.3	5.1	6.6

TABLE S.14: Rankings of the nine approximated optimal μ-distributions ($\boldsymbol{A}_{\text{HV}}$, ..., $\boldsymbol{A}_{\text{PD}}$) by each quality indicator on F_{convex} with $m = 5$.

	$\boldsymbol{A}_{\text{HV}}$	$\boldsymbol{A}_{\text{IGD}}$	$\boldsymbol{A}_{\text{IGD+}}$	$\boldsymbol{A}_{\text{R2}}$	$\boldsymbol{A}_{\text{NR2}}$	$\boldsymbol{A}_{I_{\epsilon+}}$	$\boldsymbol{A}_{\text{SE}}$	$\boldsymbol{A}_{\Delta}$	$\boldsymbol{A}_{\text{PD}}$
HV	1	7	9	6	2	8	5	3	4
IGD	7	1	2	6	8	4	9	5	3
IGD$^+$	6	4	1	3	8	2	9	7	5
R2	2	8	7	1	4	9	3	6	5
NR2	2	7	8	6	1	9	3	4	5
$I_{\epsilon+}$	5	4	2	3	8	1	9	7	6
SE	2	6	7	8	4	9	1	3	5
Δ	3	5	7	9	4	8	1	2	6
PD	3	4	8	5	6	7	9	2	1
Avg.	3.4	5.1	5.7	5.2	5.0	6.3	5.4	4.3	4.4

TABLE S.15: Rankings of the nine approximated optimal μ-distributions ($\boldsymbol{A}_{\mathrm{HV}}$, ..., $\boldsymbol{A}_{\mathrm{PD}}$) by each quality indicator on $F_{\text{i-linear}}$ with $m = 5$.

	$\boldsymbol{A}_{\mathrm{HV}}$	$\boldsymbol{A}_{\mathrm{IGD}}$	$\boldsymbol{A}_{\mathrm{IGD+}}$	$\boldsymbol{A}_{\mathrm{R2}}$	$\boldsymbol{A}_{\mathrm{NR2}}$	$\boldsymbol{A}_{I_{\epsilon+}}$	$\boldsymbol{A}_{\mathrm{SE}}$	$\boldsymbol{A}_{\Delta}$	$\boldsymbol{A}_{\mathrm{PD}}$
HV	1	4	2	9	3	6	8	7	5
IGD	3	1	2	8	4	6	9	7	5
IGD$^+$	3	2	1	9	4	6	8	7	5
R2	6	9	8	1	4	3	2	5	7
NR2	2	6	3	8	1	4	9	7	5
$I_{\epsilon+}$	6	8	5	3	2	1	4	7	9
SE	6	9	7	2	3	5	1	4	8
Δ	5	7	6	4	3	9	2	1	8
PD	2	7	6	8	5	3	9	4	1
Avg.	3.8	5.9	4.4	5.8	3.2	4.8	5.8	5.4	5.9

TABLE S.16: Rankings of the nine approximated optimal μ-distributions ($\boldsymbol{A}_{\mathrm{HV}}$, ..., $\boldsymbol{A}_{\mathrm{PD}}$) by each quality indicator on $F_{\text{i-concave}}$ with $m = 5$.

	$\boldsymbol{A}_{\mathrm{HV}}$	$\boldsymbol{A}_{\mathrm{IGD}}$	$\boldsymbol{A}_{\mathrm{IGD+}}$	$\boldsymbol{A}_{\mathrm{R2}}$	$\boldsymbol{A}_{\mathrm{NR2}}$	$\boldsymbol{A}_{I_{\epsilon+}}$	$\boldsymbol{A}_{\mathrm{SE}}$	$\boldsymbol{A}_{\Delta}$	$\boldsymbol{A}_{\mathrm{PD}}$
HV	1	9	5	3	2	6	4	7	8
IGD	6	1	4	7	8	5	9	3	2
IGD$^+$	2	8	1	3	4	7	9	6	5
R2	3	8	6	1	2	5	4	7	9
NR2	2	9	5	3	1	6	4	7	8
$I_{\epsilon+}$	2	8	6	1	3	5	4	7	9
SE	3	9	6	4	2	8	1	5	7
Δ	2	7	6	3	4	9	1	5	8
PD	8	4	5	7	9	3	6	2	1
Avg.	3.2	7.0	4.9	3.6	3.9	6.0	4.7	5.4	6.3

TABLE S.17: Rankings of the nine approximated optimal μ-distributions ($\boldsymbol{A}_{\mathrm{HV}}$, ..., $\boldsymbol{A}_{\mathrm{PD}}$) by each quality indicator on $F_{\text{i-convex}}$ with $m = 5$.

	$\boldsymbol{A}_{\mathrm{HV}}$	$\boldsymbol{A}_{\mathrm{IGD}}$	$\boldsymbol{A}_{\mathrm{IGD+}}$	$\boldsymbol{A}_{\mathrm{R2}}$	$\boldsymbol{A}_{\mathrm{NR2}}$	$\boldsymbol{A}_{I_{\epsilon+}}$	$\boldsymbol{A}_{\mathrm{SE}}$	$\boldsymbol{A}_{\Delta}$	$\boldsymbol{A}_{\mathrm{PD}}$
HV	1	7	3	5	2	4	9	8	6
IGD	8	1	4	2	7	9	6	5	3
IGD$^+$	2	7	1	5	3	4	9	8	6
R2	4	3	2	1	5	7	8	9	6
NR2	2	7	3	5	1	4	9	8	6
$I_{\epsilon+}$	2	8	4	6	3	1	9	7	5
SE	9	3	6	4	8	7	1	2	5
Δ	7	3	5	6	9	8	2	1	4
PD	8	7	6	3	5	2	9	4	1
Avg.	4.8	5.1	3.8	4.1	4.8	5.1	6.9	5.8	4.7

TABLE S.18: Rankings of the nine approximated optimal μ-distributions ($\boldsymbol{A}_{\mathrm{HV}}$, ..., $\boldsymbol{A}_{\mathrm{PD}}$) by each quality indicator on F_{linear} with $m = 8$.

	$\boldsymbol{A}_{\mathrm{HV}}$	$\boldsymbol{A}_{\mathrm{IGD}}$	$\boldsymbol{A}_{\mathrm{IGD+}}$	$\boldsymbol{A}_{\mathrm{R2}}$	$\boldsymbol{A}_{\mathrm{NR2}}$	$\boldsymbol{A}_{I_{\epsilon+}}$	$\boldsymbol{A}_{\mathrm{SE}}$	$\boldsymbol{A}_{\Delta}$	$\boldsymbol{A}_{\mathrm{PD}}$
HV	1	8	9	6	3	7	2	4	5
IGD	7	1	2	3	8	6	9	5	4
IGD$^+$	7	2	1	4	8	3	9	6	5
R2	2	7	8	1	4	9	3	5	6
NR2	6	5	4	7	1	9	2	3	8
$I_{\epsilon+}$	7	2	3	4	8	1	9	6	5
SE	2	7	8	6	5	9	1	3	4
Δ	3	5	7	9	4	8	1	2	6
PD	8	6	7	3	5	4	9	2	1
Avg.	4.8	4.8	5.4	4.8	5.1	6.2	5.0	4.0	4.9

TABLE S.19: Rankings of the nine approximated optimal μ-distributions ($\boldsymbol{A}_{\mathrm{HV}}$, ..., $\boldsymbol{A}_{\mathrm{PD}}$) by each quality indicator on F_{concave} with $m = 8$.

	$\boldsymbol{A}_{\mathrm{HV}}$	$\boldsymbol{A}_{\mathrm{IGD}}$	$\boldsymbol{A}_{\mathrm{IGD}^+}$	$\boldsymbol{A}_{\mathrm{R2}}$	$\boldsymbol{A}_{\mathrm{NR2}}$	$\boldsymbol{A}_{I_{\epsilon+}}$	$\boldsymbol{A}_{\mathrm{SE}}$	$\boldsymbol{A}_{\Delta}$	$\boldsymbol{A}_{\mathrm{PD}}$
HV	1	9	2	5	4	8	3	6	7
IGD	9	1	6	5	7	2	8	4	3
IGD$^+$	2	6	1	5	4	8	7	3	9
R2	2	9	4	1	3	8	5	6	7
NR2	2	9	3	6	1	8	4	5	7
$I_{\epsilon+}$	6	2	4	8	3	1	9	5	7
SE	2	8	4	3	6	9	1	5	7
Δ	2	7	3	4	6	9	5	1	8
PD	9	5	7	4	6	2	8	3	1
Avg.	3.9	6.2	3.8	4.6	4.4	6.1	5.6	4.2	6.2

TABLE S.20: Rankings of the nine approximated optimal μ-distributions ($\boldsymbol{A}_{\mathrm{HV}}$, ..., $\boldsymbol{A}_{\mathrm{PD}}$) by each quality indicator on F_{convex} with $m = 8$.

	$\boldsymbol{A}_{\mathrm{HV}}$	$\boldsymbol{A}_{\mathrm{IGD}}$	$\boldsymbol{A}_{\mathrm{IGD}^+}$	$\boldsymbol{A}_{\mathrm{R2}}$	$\boldsymbol{A}_{\mathrm{NR2}}$	$\boldsymbol{A}_{I_{\epsilon+}}$	$\boldsymbol{A}_{\mathrm{SE}}$	$\boldsymbol{A}_{\Delta}$	$\boldsymbol{A}_{\mathrm{PD}}$
HV	1	7	9	6	2	8	5	4	3
IGD	8	1	3	5	6	7	9	4	2
IGD$^+$	8	3	1	2	6	4	9	7	5
R2	4	5	3	1	2	8	9	7	6
NR2	5	4	3	2	1	6	9	8	7
$I_{\epsilon+}$	8	2	3	4	6	1	9	7	5
SE	2	4	7	8	5	9	1	3	6
Δ	2	4	6	9	8	7	1	3	5
PD	6	5	8	3	4	7	9	2	1
Avg.	4.9	3.9	4.8	4.4	4.4	6.3	6.8	5.0	4.4

TABLE S.21: Rankings of the nine approximated optimal μ-distributions ($\boldsymbol{A}_{\mathrm{HV}}$, ..., $\boldsymbol{A}_{\mathrm{PD}}$) by each quality indicator on $F_{\text{i-linear}}$ with $m = 8$.

	$\boldsymbol{A}_{\mathrm{HV}}$	$\boldsymbol{A}_{\mathrm{IGD}}$	$\boldsymbol{A}_{\mathrm{IGD}^+}$	$\boldsymbol{A}_{\mathrm{R2}}$	$\boldsymbol{A}_{\mathrm{NR2}}$	$\boldsymbol{A}_{I_{\epsilon+}}$	$\boldsymbol{A}_{\mathrm{SE}}$	$\boldsymbol{A}_{\Delta}$	$\boldsymbol{A}_{\mathrm{PD}}$
HV	1	5	2	8	4	6	9	7	3
IGD	4	1	2	8	3	6	9	7	5
IGD$^+$	3	2	1	8	4	5	9	7	6
R2	8	7	5	1	6	4	2	3	9
NR2	4	2	3	7	1	6	9	8	5
$I_{\epsilon+}$	7	6	5	2	8	1	3	4	9
SE	4	8	6	2	9	5	1	3	7
Δ	4	6	5	3	9	7	1	2	8
PD	2	8	5	6	7	3	9	4	1
Avg.	4.1	5.0	3.8	5.0	5.7	4.8	5.8	5.0	5.9

TABLE S.22: Rankings of the nine approximated optimal μ-distributions ($\boldsymbol{A}_{\mathrm{HV}}$, ..., $\boldsymbol{A}_{\mathrm{PD}}$) by each quality indicator on $F_{\text{i-concave}}$ with $m = 8$.

	$\boldsymbol{A}_{\mathrm{HV}}$	$\boldsymbol{A}_{\mathrm{IGD}}$	$\boldsymbol{A}_{\mathrm{IGD}^+}$	$\boldsymbol{A}_{\mathrm{R2}}$	$\boldsymbol{A}_{\mathrm{NR2}}$	$\boldsymbol{A}_{I_{\epsilon+}}$	$\boldsymbol{A}_{\mathrm{SE}}$	$\boldsymbol{A}_{\Delta}$	$\boldsymbol{A}_{\mathrm{PD}}$
HV	1	7	5	4	3	6	2	8	9
IGD	8	1	4	6	7	3	9	5	2
IGD$^+$	5	6	1	2	3	4	7	8	9
R2	2	7	5	1	4	6	3	8	9
NR2	1	7	5	4	2	6	3	8	9
$I_{\epsilon+}$	2	7	6	1	4	5	3	8	9
SE	2	8	6	5	3	9	1	4	7
Δ	2	7	6	8	3	9	1	4	5
PD	9	4	6	5	7	3	8	2	1
Avg.	3.6	6.0	4.9	4.0	4.0	5.7	4.1	6.1	6.7

TABLE S.23: Rankings of the nine approximated optimal μ-distributions ($\boldsymbol{A}_{\mathrm{HV}}$, ..., $\boldsymbol{A}_{\mathrm{PD}}$) by each quality indicator on $F_{\text{i-convex}}$ with $m = 8$.

	$\boldsymbol{A}_{\mathrm{HV}}$	$\boldsymbol{A}_{\mathrm{IGD}}$	$\boldsymbol{A}_{\mathrm{IGD+}}$	$\boldsymbol{A}_{\mathrm{R2}}$	$\boldsymbol{A}_{\mathrm{NR2}}$	$\boldsymbol{A}_{I_{\epsilon+}}$	$\boldsymbol{A}_{\mathrm{SE}}$	$\boldsymbol{A}_{\Delta}$	$\boldsymbol{A}_{\mathrm{PD}}$
HV	1	6	3	5	2	4	9	8	7
IGD	8	1	3	2	7	5	9	4	6
IGD$^+$	3	5	1	6	2	4	9	8	7
R2	9	6	2	1	5	3	7	8	4
NR2	3	6	2	5	1	4	9	8	7
$I_{\epsilon+}$	4	7	2	5	3	1	8	9	6
SE	8	5	7	3	9	6	1	2	4
Δ	8	3	6	4	9	7	2	1	5
PD	5	6	7	4	8	2	9	3	1
Avg.	5.4	5.0	3.7	3.9	5.1	4.0	7.0	5.7	5.2

TABLE S.24: Kendall rank correlation τ values of the nine quality indicator on F_{linear} with $m = 5$.

	HV	IGD	IGD$^+$	R2	NR2	$I_{\epsilon+}$	SE	Δ	PD
HV	1.00	-0.67	-0.78	0.33	0.89	-0.67	0.67	0.17	-0.06
IGD	-0.67	1.00	0.89	-0.33	-0.67	0.67	-0.56	-0.06	0.39
IGD$^+$	-0.78	0.89	1.00	-0.44	-0.78	0.67	-0.67	-0.17	0.28
R2	0.33	-0.33	-0.44	1.00	0.44	-0.56	0.67	0.39	-0.17
NR2	0.89	-0.67	-0.78	0.44	1.00	-0.56	0.67	0.17	-0.17
$I_{\epsilon+}$	-0.67	0.67	0.67	-0.56	-0.56	1.00	-0.89	-0.39	0.28
SE	0.67	-0.56	-0.67	0.67	0.67	-0.89	1.00	0.50	-0.28
Δ	0.17	-0.06	-0.17	0.39	0.17	-0.39	0.50	1.00	-0.22
PD	-0.06	0.39	0.28	-0.17	-0.17	0.28	-0.28	-0.22	1.00

TABLE S.25: Kendall rank correlation τ values of the nine quality indicator on F_{concave} with $m = 5$.

	HV	IGD	IGD$^+$	R2	NR2	$I_{\epsilon+}$	SE	Δ	PD
HV	1.00	-0.83	0.67	0.67	0.78	0.00	0.39	0.00	-0.67
IGD	-0.83	1.00	-0.61	-0.61	-0.72	0.06	-0.22	0.06	0.61
IGD$^+$	0.67	-0.61	1.00	0.56	0.67	0.11	0.50	0.00	-0.78
R2	0.67	-0.61	0.56	1.00	0.67	0.00	0.28	0.00	-0.44
NR2	0.78	-0.72	0.67	0.67	1.00	-0.11	0.50	0.11	-0.56
$I_{\epsilon+}$	0.00	0.06	0.11	0.00	-0.11	1.00	-0.28	-0.56	-0.22
SE	0.39	-0.22	0.50	0.28	0.50	-0.28	1.00	0.50	-0.39
Δ	0.00	0.06	0.00	0.00	0.11	-0.56	0.50	1.00	0.11
PD	-0.67	0.61	-0.78	-0.44	-0.56	-0.22	-0.39	0.11	1.00

TABLE S.26: Kendall rank correlation τ values of the nine quality indicator on F_{convex} with $m = 5$.

	HV	IGD	IGD$^+$	R2	NR2	$I_{\epsilon+}$	SE	Δ	PD
HV	1.00	-0.44	-0.61	0.39	0.78	-0.50	0.56	0.39	0.33
IGD	-0.44	1.00	0.61	-0.50	-0.56	0.50	-0.44	-0.28	0.22
IGD$^+$	-0.61	0.61	1.00	-0.33	-0.72	0.89	-0.72	-0.67	-0.17
R2	0.39	-0.50	-0.33	1.00	0.50	-0.33	0.39	0.22	0.06
NR2	0.78	-0.56	-0.72	0.50	1.00	-0.72	0.67	0.50	0.11
$I_{\epsilon+}$	-0.50	0.50	0.89	-0.33	-0.72	1.00	-0.72	-0.67	-0.17
SE	0.56	-0.44	-0.72	0.39	0.67	-0.72	1.00	0.83	0.11
Δ	0.39	-0.28	-0.67	0.22	0.50	-0.67	0.83	1.00	0.06
PD	0.33	0.22	-0.17	0.06	0.11	-0.17	0.11	0.06	1.00

TABLE S.27: Kendall rank correlation τ values of the nine quality indicator on $F_{\text{i-linear}}$ with $m = 5$.

	HV	IGD	IGD$^+$	R2	NR2	$I_{\epsilon+}$	SE	Δ	PD
HV	1.00	0.72	0.83	-0.56	0.67	-0.17	-0.44	-0.06	0.33
IGD	0.72	1.00	0.89	-0.72	0.50	-0.22	-0.72	-0.33	0.17
IGD$^+$	0.83	0.89	1.00	-0.72	0.50	-0.22	-0.61	-0.22	0.17
R2	-0.56	-0.72	-0.72	1.00	-0.22	0.50	0.78	0.28	-0.22
NR2	0.67	0.50	0.50	-0.22	1.00	0.06	-0.22	-0.17	0.44
$I_{\epsilon+}$	-0.17	-0.22	-0.22	0.50	0.06	1.00	0.39	0.11	-0.17
SE	-0.44	-0.72	-0.61	0.78	-0.22	0.39	1.00	0.50	-0.44
Δ	-0.06	-0.33	-0.22	0.28	-0.17	0.11	0.50	1.00	-0.28
PD	0.33	0.17	0.17	-0.22	0.44	-0.17	-0.44	-0.28	1.00

TABLE S.28: Kendall rank correlation τ values of the nine quality indicator on $F_{\text{i-concave}}$ with $m = 5$.

	HV	IGD	IGD$^+$	R2	NR2	$I_{\epsilon+}$	SE	Δ	PD
HV	1.00	-0.67	0.33	0.72	0.94	0.78	0.61	0.50	-0.78
IGD	-0.67	1.00	0.00	-0.72	-0.72	-0.67	-0.72	-0.50	0.56
IGD$^+$	0.33	0.00	1.00	0.17	0.28	0.22	0.17	0.17	-0.11
R2	0.72	-0.72	0.17	1.00	0.78	0.94	0.44	0.44	-0.72
NR2	0.94	-0.72	0.28	0.78	1.00	0.72	0.67	0.44	-0.83
$I_{\epsilon+}$	0.78	-0.67	0.22	0.94	0.72	1.00	0.39	0.50	-0.67
SE	0.61	-0.72	0.17	0.44	0.67	0.39	1.00	0.78	-0.50
Δ	0.50	-0.50	0.17	0.44	0.44	0.50	0.78	1.00	-0.50
PD	-0.78	0.56	-0.11	-0.72	-0.83	-0.67	-0.50	-0.50	1.00

TABLE S.29: Kendall rank correlation τ values of the nine quality indicator on $F_{\text{i-convex}}$ with $m = 5$.

	HV	IGD	IGD$^+$	R2	NR2	$I_{\epsilon+}$	SE	Δ	PD
HV	1.00	-0.28	0.89	0.33	0.94	0.72	-0.89	-0.72	0.00
IGD	-0.28	1.00	-0.17	0.28	-0.22	-0.56	0.39	0.33	0.06
IGD$^+$	0.89	-0.17	1.00	0.44	0.83	0.61	-0.78	-0.61	0.00
R2	0.33	0.28	0.44	1.00	0.28	0.06	-0.22	-0.28	0.00
NR2	0.94	-0.22	0.83	0.28	1.00	0.67	-0.83	-0.78	0.06
$I_{\epsilon+}$	0.72	-0.56	0.61	0.06	0.67	1.00	-0.83	-0.67	0.28
SE	-0.89	0.39	-0.78	-0.22	-0.83	-0.83	1.00	0.72	-0.11
Δ	-0.72	0.33	-0.61	-0.28	-0.78	-0.67	0.72	1.00	-0.17
PD	0.00	0.06	0.00	0.00	0.06	0.28	-0.11	-0.17	1.00

TABLE S.30: Kendall rank correlation τ values of the nine quality indicator on F_{linear} with $m = 8$.

	HV	IGD	IGD$^+$	R2	NR2	$I_{\epsilon+}$	SE	Δ	PD
HV	1.00	-0.67	-0.89	0.61	0.22	-0.72	0.72	0.50	-0.06
IGD	-0.67	1.00	0.78	-0.28	-0.22	0.72	-0.50	-0.39	0.28
IGD$^+$	-0.89	0.78	1.00	-0.50	-0.33	0.83	-0.72	-0.50	0.06
R2	0.61	-0.28	-0.50	1.00	0.17	-0.56	0.56	0.33	-0.11
NR2	0.22	-0.22	-0.33	0.17	1.00	-0.50	0.28	0.50	-0.28
$I_{\epsilon+}$	-0.72	0.72	0.83	-0.56	-0.50	1.00	-0.78	-0.56	0.22
SE	0.72	-0.50	-0.72	0.56	0.28	-0.78	1.00	0.67	-0.11
Δ	0.50	-0.39	-0.50	0.33	0.50	-0.56	0.67	1.00	-0.33
PD	-0.06	0.28	0.06	-0.11	-0.28	0.22	-0.11	-0.33	1.00

TABLE S.31: Kendall rank correlation τ values of the nine quality indicator on F_{concave} with $m = 8$.

	HV	IGD	IGD$^+$	R2	NR2	$I_{\epsilon+}$	SE	Δ	PD
HV	1.00	-0.89	0.44	0.67	0.78	-0.33	0.67	0.50	-0.67
IGD	-0.89	1.00	-0.33	-0.67	-0.78	0.33	-0.67	-0.39	0.67
IGD$^+$	0.44	-0.33	1.00	0.33	0.44	0.00	0.33	0.61	-0.44
R2	0.67	-0.67	0.33	1.00	0.67	-0.33	0.56	0.39	-0.33
NR2	0.78	-0.78	0.44	0.67	1.00	-0.11	0.44	0.39	-0.44
$I_{\epsilon+}$	-0.33	0.33	0.00	-0.33	-0.11	1.00	-0.67	-0.28	0.22
SE	0.67	-0.67	0.33	0.56	0.44	-0.67	1.00	0.50	-0.56
Δ	0.50	-0.39	0.61	0.39	0.39	-0.28	0.50	1.00	-0.39
PD	-0.67	0.67	-0.44	-0.33	-0.44	0.22	-0.56	-0.39	1.00

TABLE S.32: Kendall rank correlation τ values of the nine quality indicator on F_{convex} with $m = 8$.

	HV	IGD	IGD$^+$	R2	NR2	$I_{\epsilon+}$	SE	Δ	PD
HV	1.00	-0.22	-0.50	0.11	0.00	-0.56	0.39	0.17	0.33
IGD	-0.22	1.00	0.50	0.22	0.11	0.44	-0.17	-0.17	0.44
IGD$^+$	-0.50	0.50	1.00	0.39	0.50	0.72	-0.67	-0.56	0.06
R2	0.11	0.22	0.39	1.00	0.78	0.11	-0.28	-0.50	0.22
NR2	0.00	0.11	0.50	0.78	1.00	0.22	-0.39	-0.61	0.11
$I_{\epsilon+}$	-0.56	0.44	0.72	0.11	0.22	1.00	-0.72	-0.50	0.00
SE	0.39	-0.17	-0.67	-0.28	-0.39	-0.72	1.00	0.78	-0.17
Δ	0.17	-0.17	-0.56	-0.50	-0.61	-0.50	0.78	1.00	-0.28
PD	0.33	0.44	0.06	0.22	0.11	0.00	-0.17	-0.28	1.00

TABLE S.33: Kendall rank correlation τ values of the nine quality indicator on $F_{\text{i-linear}}$ with $m = 8$.

	HV	IGD	IGD$^+$	R2	NR2	$I_{\epsilon+}$	SE	Δ	PD
HV	1.00	0.61	0.67	-0.67	0.56	-0.50	-0.44	-0.33	0.44
IGD	0.61	1.00	0.83	-0.50	0.83	-0.33	-0.72	-0.50	0.06
IGD$^+$	0.67	0.83	1.00	-0.44	0.67	-0.17	-0.56	-0.33	0.11
R2	-0.67	-0.50	-0.44	1.00	-0.44	0.72	0.56	0.44	-0.33
NR2	0.56	0.83	0.67	-0.44	1.00	-0.39	-0.78	-0.67	0.00
$I_{\epsilon+}$	-0.50	-0.33	-0.17	0.72	-0.39	1.00	0.50	0.39	-0.17
SE	-0.44	-0.72	-0.56	0.56	-0.78	0.50	1.00	0.78	-0.11
Δ	-0.33	-0.50	-0.33	0.44	-0.67	0.39	0.78	1.00	-0.22
PD	0.44	0.06	0.11	-0.33	0.00	-0.17	-0.11	-0.22	1.00

TABLE S.34: Kendall rank correlation τ values of the nine quality indicator on $F_{\text{i-concave}}$ with $m = 8$.

	HV	IGD	IGD$^+$	R2	NR2	$I_{\epsilon+}$	SE	Δ	PD
HV	1.00	-0.72	0.33	0.83	0.94	0.78	0.56	0.33	-0.89
IGD	-0.72	1.00	-0.06	-0.56	-0.67	-0.50	-0.83	-0.61	0.61
IGD$^+$	0.33	-0.06	1.00	0.50	0.39	0.44	-0.11	-0.22	-0.33
R2	0.83	-0.56	0.50	1.00	0.78	0.94	0.39	0.17	-0.72
NR2	0.94	-0.67	0.39	0.78	1.00	0.72	0.50	0.28	-0.83
$I_{\epsilon+}$	0.78	-0.50	0.44	0.94	0.72	1.00	0.33	0.11	-0.67
SE	0.56	-0.83	-0.11	0.39	0.50	0.33	1.00	0.78	-0.56
Δ	0.33	-0.61	-0.22	0.17	0.28	0.11	0.78	1.00	-0.44
PD	-0.89	0.61	-0.33	-0.72	-0.83	-0.67	-0.56	-0.44	1.00

TABLE S.35: Kendall rank correlation τ values of the nine quality indicator on $F_{\text{i-convex}}$ with $m = 8$.

	HV	IGD	IGD$^+$	R2	NR2	$I_{\epsilon+}$	SE	Δ	PD
HV	1.00	-0.11	0.78	0.11	0.89	0.56	-0.83	-0.72	-0.11
IGD	-0.11	1.00	0.11	0.44	0.00	0.00	0.06	0.28	0.11
IGD$^+$	0.78	0.11	1.00	0.22	0.89	0.67	-0.83	-0.61	-0.22
R2	0.11	0.44	0.22	1.00	0.22	0.44	-0.06	-0.17	0.11
NR2	0.89	0.00	0.89	0.22	1.00	0.67	-0.83	-0.72	-0.22
$I_{\epsilon+}$	0.56	0.00	0.67	0.44	0.67	1.00	-0.50	-0.72	0.00
SE	-0.83	0.06	-0.83	-0.06	-0.83	-0.50	1.00	0.78	0.17
Δ	-0.72	0.28	-0.61	-0.17	-0.72	-0.72	0.78	1.00	0.06
PD	-0.11	0.11	-0.22	0.11	-0.22	0.00	0.17	0.06	1.00

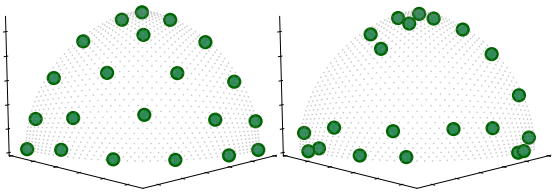

(a) $\boldsymbol{A}_{\mathrm{DCI21}}$ (b) $\boldsymbol{A}_{\mathrm{DCI28}}$

Fig. S.51: Distribution of objective vectors in $\boldsymbol{A}_{\mathrm{DCI21}}$ and $\boldsymbol{A}_{\mathrm{DCI28}}$ with $\mu = 21$ on F_{concave}.

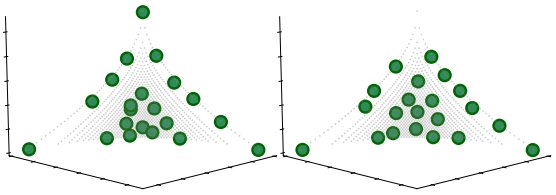

(a) $\boldsymbol{A}_{\mathrm{DCI21}}$ (b) $\boldsymbol{A}_{\mathrm{DCI28}}$

Fig. S.52: Distribution of objective vectors in $\boldsymbol{A}_{\mathrm{DCI21}}$ and $\boldsymbol{A}_{\mathrm{DCI28}}$ with $\mu = 21$ on F_{convex}.

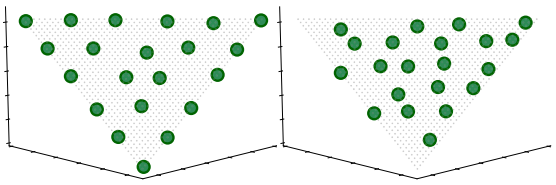

(a) $\boldsymbol{A}_{\mathrm{DCI21}}$ (b) $\boldsymbol{A}_{\mathrm{DCI28}}$

Fig. S.53: Distribution of objective vectors in $\boldsymbol{A}_{\mathrm{DCI21}}$ and $\boldsymbol{A}_{\mathrm{DCI28}}$ with $\mu = 21$ on $F_{\mathrm{i\text{-}linear}}$.

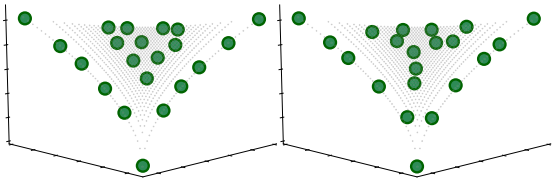

(a) $\boldsymbol{A}_{\mathrm{DCI21}}$ (b) $\boldsymbol{A}_{\mathrm{DCI28}}$

Fig. S.54: Distribution of objective vectors in $\boldsymbol{A}_{\mathrm{DCI21}}$ and $\boldsymbol{A}_{\mathrm{DCI28}}$ with $\mu = 21$ on $F_{\mathrm{i\text{-}concave}}$.

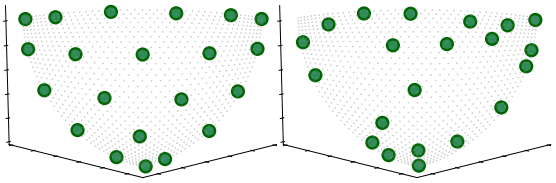

(a) $\boldsymbol{A}_{\mathrm{DCI21}}$ (b) $\boldsymbol{A}_{\mathrm{DCI28}}$

Fig. S.55: Distribution of objective vectors in $\boldsymbol{A}_{\mathrm{DCI21}}$ and $\boldsymbol{A}_{\mathrm{DCI28}}$ with $\mu = 21$ on $F_{\mathrm{i\text{-}convex}}$.